BearWorks

MSU Graduate Theses

Spring 2018

Enhanced Production of Pro-IL-1**B**eta Contributes to Immunopathology during the Coinfection of Influenza a Virus and Streptococcus Pneumoniae

Angeline E. Rodriguez
Missouri State University, Rodriguez281@live.missouristate.edu

Follow this and additional works at: https://bearworks.missouristate.edu/theses

Part of the Bacterial Infections and Mycoses Commons, Biology Commons, Immunity Commons, Immunology of Infectious Disease Commons, Immunopathology Commons, Medical Immunology Commons, Other Immunology and Infectious Disease Commons, and the Virus Diseases Commons

Recommended Citation
Rodriguez, Angeline E., "Enhanced Production of Pro-IL-1Beta Contributes to Immunopathology during the Coinfection of Influenza a Virus and Streptococcus Pneumoniae" (2018). *MSU Graduate Theses*. 3242.
https://bearworks.missouristate.edu/theses/3242

ENHANCED PRODUCTION OF PRO-IL-1BETA CONTRIBUTES TO

IMMUNOPATHOLOGY DURING THE COINFECTION OF INFLUENZA A

VIRUS AND *STREPTOCOCCUS PNEUMONIAE*

A Masters Thesis

Presented to

The Graduate College of

Missouri State University

In Partial Fulfillment

Of the Requirements for the Degree

Master of Science, Biology

By

Angeline Ernestina Rodriguez

May 2018

ENHANCED PRODUCTION OF PRO-IL-1BETA CONTRIBUTES TO IMMUNOPATHOLOGY DURING THE COINFECTION OF INFLUENZA A VIRUS AND *STREPTOCOCCUS PNEUMONIAE*

Biology

Missouri State University, May 2018

Master of Science

Angeline Ernestina Rodriguez

ABSTRACT

Viral bacterial coinfections are known to cause severe pneumonia, especially in the elderly and in pediatric patients. Antibiotics like β-Lactams kill the bacteria but fail to improve symptoms suggesting a faulty immune system may play an important role in the disease. Interleukin-1β (IL-1β) is an important immune signaling cytokine responsible for inflammation. It exists as an inactive precursor that can be activated by caspase-1 containing inflammasomes (multi-protein complex). Influenza A virus (IAV) and *Streptococcus pneumoniae* (*S. pneumoniae*) activate the inflammasome through the NOD-like receptor protein NLRP3 and/or AIM2. Previous reports in mice indicate that IL-1β levels are dramatically elevated during coinfection with IAV and *S. pneumoniae.* However, how IL-1β levels increase and their importance in coinfection is not known. We have discovered that IL-1β expression and secretion is increased during coinfection as a result of activation of multiple signaling pathways simultaneously. This was concluded in experiments where macrophages or mice deficient in various immune pathways including *Myd88*, *Aim2* or *Nlrp3* genes were examined for their effects on IL-1β production. Treatment options were then explored. Mice were given an antibiotic and/or an IL-1β neutralizing antibody. Treatment of mice with clindamycin antibiotic significantly improved mortality and simultaneously reduced IL-1β levels. Further inhibition of IL-1β using neutralizing antibodies resulted in improved weight gain compared to clindamycin alone. Thus, we concluded that IL-1β plays an important role during the coinfection of IAV and *S. pneumoniae.*

This abstract is approved as to form and content

_____
Christopher Lupfer, PhD
Chairperson, Advisory Committee
Missouri State University

ENHANCED PRODUCTION OF PRO-IL-1BETA CONTRIBUTES TO

IMMUNOPATHOLOGY DURING THE COINFECTION OF INFLUENZA A

VIRUS AND *STREPTOCOCCUS PNEUMONIAE*

By

Angeline Ernestina Rodriguez

A Masters Thesis
Submitted to the Graduate College
Of Missouri State University
In Partial Fulfillment of the Requirements
For the Degree of Masters of Science, Biology

May 2018

Approved:

_____
Christopher Lupfer, PhD

_____
Ryan Udan, PhD

_____
Kyoungtae Kim, PhD

_____
Julie Masterson, PhD: Dean, Graduate College

ACKNOWLEDGEMENTS

TABLE OF CONTENTS

LIST OF TABLES

LIST OF FIGURES

INTRODUCTION

A coinfection occurs when the host is infected by one pathogen, which initiates an immune response and taxes the body's resources. A second pathogen then takes advantage of this weakness and also attacks the host (1). Secondary bacterial infection during influenza A virus (IAV) infection is a contributing factor to disease severity and mortality. *Streptococcus pneumoniae (S. pneumoniae)* is one of the main pathogens causing coinfection following IAV infection (2-4). In fact, the coinfection of IAV and *S. pneumoniae* is the 8th leading cause of death in the United States (5). Throughout history, influenza pandemics have taken millions of lives. The highest mortality was recorded in the 1918-1919 H1N1 "Spanish flu" pandemic, which resulted in 50-100 million deaths (6-8). Autopsies of Spanish flu victims linked the deaths to severe complications related to bacterial coinfections, with *S. pneumoniae* as a major coinfecting agent (9-12). Subsequent research has shown that infection with more severe IAV strains leads to increased susceptibility to bacterial coinfections (8, 13, 14). In this particular coinfection, the immune system response plays an important role in the development of disease. In part, the response of the immune system to IAV is different than the one to *S. pneumoniae*. Thus, when a coinfection occurs, the immune response to IAV impairs the response to *S. pneumoniae.* Therefore, to understand coinfection, one must first understand the pathogens involved and the immune response to those pathogens. Our hope is that a better understanding of the mechanisms responsible for this coinfection can facilitate the quality of treatment available.

Influenza A Virus

IAV is an enveloped negative-sense single-stranded RNA virus part of the Orthomyxoviridae family (15). Its genome is made up of eight RNA segments that can encode up to 12 different proteins. There are two types of glycoproteins, hemagglutinin (HA) and neuraminidase (NA). Within those two groups, there are 17 subtypes of HA (H1–H17) and 9 of NA (N1-N9) (16-18). Additional proteins include the matrix proteins 1 and 2 (M1 and M2) (19), nucleoprotein (NP) (20), polymerase complex proteins (Phox and Bem1/2 (PB1, PB2,) and Polymerase acidic protein (PA)) (21, 22), and non-structural proteins 1/2 (NS1 (23), NS2 (24, 25),), PA-X (26) and PB1-F2 (27). There are four types of influenza viruses (A, B, C, D) (28-30). Influenza types A, B and C originate from avian, mammal and human sources and all three are able to cause infection in humans, with influenza A virus producing the most severe disease and influenza C virus the least severe (31-33). Influenza D virus thus far has only been detected in cattle (30). The influenza A virus has been seen under prevailing pandemic conditions, due to being the only strain with an animal reservoir that can transmit to humans, hence attention has mostly been focused on it (34, 35). Transmission of the virus occurs through inhalation of infectious air droplets and contact with infected fomites (36). Once inside the body, the virus infects columnar epithelial cells in the respiratory tract by the attachment of HA to specific sialic acid residues, which are present on the cell surface through post-translational glycosylation modifications on cell proteins destined for the cell surface. Binding to sialic acid induces Clathrin mediated endocytosis (CME) or other alternative endocytic routes, which allows the virus to enter the cell (37, 38). Once the virus is in the endosome, M2 proteins allow H^+ ion influx and cause dissociation of M1 proteins from

nucleocapsids. Viral and endosomal membrane fusion through changes in the HA protein

conformation also occur (39). The viral ribonucleoprotein particles (vRNPs) made up of

viral genomic RNA (vRNA), PB1, PB2, PA, and NP are released into the cytoplasm and

translocate to the nucleus to begin replication and transcription (40, 41). When the

vRNPs enter the nucleus, transcription of positive sense viral mRNA begins (42, 43).

Transcription initiates when PB2 binds to the 5′-cap structure of host mRNAs, cutting it

and snatching it to allowing those ~12 nucleotides to serve as a primer template for the

polymerase acidic protein (PA) to start mRNA synthesis (44-46). The viral polymerase

also produces complementary RNA (cRNA), which is similar to mRNA, but without a

5'-cap. This cRNA is then used as a template to make the negative stranded vRNA. Once

sufficient viral proteins have been synthesized using the mRNA, the virus polymerase

switches to the production of vRNA. vRNA exits the nucleus and M1 proteins package

the virus so it can be ready to exit the cell (47). Newly packed virions then assemble at

the plasma membrane and initiate a process called budding (48). First, HA and NA

interact with lipid rafts (cholesterol enriched regions) in the plasma membrane allowing

the initiation of budding. Second, M1 protein is recruited and binds to the cytoplasmic

tails of HA an NA. Then vRNPs gather around the M1 protein. Third, virion elongation

occurs due to the polymerization of the M1 protein. Budding is finalized when the M1

protein recruits the M2 protein, which initiates membrane scission and viral release.

Finally, when the virus buds out of the cell, NA protein allows it to detach from sialic

acid receptors and infect new cells (49, 50) . IAV causes the disease influenza, with

symptoms consisting of fatigue, runny nose, fever, chills, headaches, muscle aches, and

congestion. IAV also allows bacteria like *S. pneumoniae* to initiate pathogenicity through multiple factors (51-55).

Streptococcus pneumoniae (S. pneumoniae)

S. pneumoniae is a non-spore forming diploccoci, characterized by its round two-joined cells that can form long chains. It is facultative anaerobic, being able to grow with or without oxygen. It is also alpha-hemolytic, so when grown on a blood agar plate, it oxidizes hemoglobin and lyses red blood cells. This type of hemolysis results in a green zone being produced around bacterial colonies. This bacterium is transformable, being able to take up genetic material from the environment. It is also nutritionally fastidious, needing specific nutrients and environmental conditions to grow. Finally, it also ferments lactic acid (56, 57). Its mode of transmission consists of droplets or aerosols distributed between hosts (58). Exposure of the host is followed by nasopharyngeal epithelial cell attachment made possible by mucosal evasion due to its capsule and neuraminidase (NanA). This leads to asymptomatic colonization in some people but systemic dissemination in others (59). This colonization is mainly found in the nasopharynx of children, yet the carriage rate decreases with age (60, 61).

S. pneumoniae is a gram-positive bacteria, and its cell wall consists of peptidoglycan and teichoic acids. A polysaccharide capsule covers the cell wall. *S. pneumoniae* virulence can be categorized by serotyping its capsular polysaccharide (62). Some serotypes act as primary pathogens and easily invade the host, yet higher mortality rates are related to opportunistic pathogens containing serotypes with lower invasive disease potential such as *S. pneumoniae* type 3 strain. The polysaccharide capsule

contains a unique teichoic acid component: a ribitol phosphate backbone that binds to phosphorylcholine (PCho) (63). PCho facilitates bacterial endocytosis, entrance into the bloodstream and crossing of other barriers due to its interaction with the platelet-activating factor receptor (PAFr) present on human cells (64). It also has pili, which aid with adhesion to human cells. Pneumococcal surface protein A (PspA), and choline binding protein (Cpb) A also aid in adherence (57). Adherence to the alveolar epithelium and the release of toxic components such as the exotoxin pneumolysin (PLY) and hydrogen peroxide results in alveolar damage and fluid build-up in the alveolar space (65, 66). PLY is a toxin produced by *S.pneumoniae* responsible for damaging the host's membrane by forming lytic pores. It has also been shown to cause DNA- double strand breaks resulting in cell cycle arrest (67). Hydrogen peroxide has been shown to be produced by *S. pneumoniae* in aerobic conditions through a pyruvate oxidase. It harms alveolar epithelial cells and other bacteria that share a common microenvironment (68).

Although *S. pneumoniae* is an extracellular pathogen that can asymptomatically colonize the upper respiratory tract, when the body is weakened, an opportunistic pathogen such as *S. pneumoniae* is able to become invasive and cause disease. *S. pneumoniae* can cause pneumonia, which is characterized by alveolar inflammation usually centering in one lobe of the lungs (69). Some of the symptoms linked to pneumonia are chills, fever, cough with phlegm or pus, and difficulty breathing. In addition to pneumonia, this pathogen is associated with otitis media, meningitis and septicemia (13, 70). These conditions are especially prominent following IAV infection and can cause the immune system to over react (13, 70).

The Immune System and Inflammation

The immune system is responsible for orchestrating cells, tissues, and organs to maintain homeostasis and defend the body against foreign agents. Inflammation is a biological response to harmful stimuli. It is characterized by five hallmarks: redness, increased heat, swelling, pain and loss of function. These five signs are due to vasodilation, increased vascular permeability, decrease cell function and increased vascularity (71). Inflammation allows the immune cells to communicate and migrate to the site of trauma. Unfortunately, if the immune system is not properly regulated, inflammation can get out of control. This can be due to intrinsic factors like genetic mutations or extrinsic factors such as coinfections (72, 73). Inflammation is initiated and regulated by the two arms of immunity: innate and adaptive.

Innate immunity is the first line of defense. If a piece of broken glass punctures the skin, the innate immune system will coordinate immune cells such as macrophages, neutrophils, eosinophils, basophils, dendritic cells and natural killer cells to arrive at the site of trauma. Macrophages are mature monocytes that patrol the vasculature and reside in tissues with the main purpose of recognizing foreign particles. They are antigen presenting cells (APCs) meaning that they travel to lymph nodes and show antigens to T cells and B cells resulting in their activation. Most resident macrophages are embryonically derived, yet others originate from hematopoietic stem cells (HSC) in the bone marrow (74). Neutrophils originate from HSC, and travel to the site of infection and produce toxic substances such as hydrogen peroxide and superoxide, and form neutrophil extracellular traps (NETs) to eliminate foreign particles. Dendritic cells are also APCs; they travel to the site of infection to gather information about the foreign agent and then

travel to the lymph nodes to present the antigen to adaptive immune cells. The innate

immune system also contains a group of proteins that make up the complement system.

These proteins help with pathogen recognition by attaching to the foreign agent. They

also surround the agent and impede its movement to other areas by a process called

opsonization. Finally, they eliminate the foreign agent by inducing cell lysis via the

membrane attack complex (75).

Specific immune receptors called Pattern Recognition Receptors (PRRs) present

on epithelial and immune cells can detect Pathogen Associated Molecular Patterns

(PAMPS), like bacterial peptidoglycan or viral RNA, or damage-associated molecular

patterns (DAMPs), like membrane damage caused by *S. pneumoniae* PLY and changes in

ion concentration occurring during infection. These PAMPS and DAMPS activate PRRs

to initiate immune signaling cascades (76, 77). All together, these cells initiate signal

transduction pathways that result in transcriptional enhancement of immune system

genes, inflammasome (multiprotein complex) activation and cytokine (immune signaling

molecules) production with the final goal of pathogen elimination and return to

homeostasis. Overall, the innate immune system has a major role in controlling

inflammation (78).

Adaptive immunity is a long-term type of immunity, it takes a few days to form,

yet long-lasting memory helps protect the body from future attacks. It is made up of the

humoral and cellular immune responses. The humoral response consists of B

lymphocytes that will produce antibodies to protect the body from future infections. The

cellular response consists of T lymphocytes that will further help with the elimination of

pathogens through receptor specificity. In the adaptive immune system, cells present

specific components from foreign particles called antigens to the receptors located on T

and B lymphocytes. This antigen presentation results in the activation, migration, and

differentiation of cells (79). During coinfection, the adaptive immune response to IAV

results in the production of specific cytokines like Interferon (IFN)-☐ that can affect the

innate immune response to the secondary infection with *S. pneumoniae* (80).

Inflammation and Immunity During Coinfection

The coinfection of IAV and *S. pneumoniae* results in pneumonia due to multiple

factors. The cooperation between coinfecting pathogens causes severe pneumonia due to

enhanced pathogen growth and dissemination as well as enhanced inflammation (81).

IAV and *S. pneumoniae* work in a synergistic manner to increase activation of PRRs

resulting in enhanced immune signaling production and inflammation.

Since the immune response to coinfection plays an important function in the

pathology of this disease, it is important to have a better understanding of the causes of

inflammation. The immune response begins when IAV initiates an infection. Then, the

virus limits some immunological mechanisms allowing *S. pneumoniae* to leave its normal

microenvironment in the pharynx and infect the lungs. If we look at this in greater detail,

the virus infects the host and spreads, causing the immune system to start trying to

eliminate it. Infected lung epithelial cells attract alveolar macrophages and monocytes

from the peripheral blood, so they can begin viral clearance through phagocytosis of

infected cells (82, 83). This intercommunication occurs through the receptor interaction

of the chemokine (C-C motif) ligand 2 (CCL2) and C-C chemokine receptor type 2

(CCR2) (84). Other cells like Natural Killer (NK) cells aid in IAV elimination through

sialylated NK Cell Activating Receptors (NKp44/ NKp46) – HA interaction (85).
Another cell type involved in the IAV immune response are dendritic cells. They can
detect IAV viral particles and mature in response to inflammatory signals. They can also
become infected by the virus or phagocytose the virus and express the viral antigens on
their cell surface through a group of proteins called Major Histocompatibility Complex
(MHC). Dendritic cells then migrate from the lungs to the lymph nodes. At the lymph
nodes, they present IAV antigens to T and B cells, which results in T cell activation or
antibody production. MHC I can activate cluster of differentiation (CD) 8$^+$ cytotoxic T
cells (CTL) (86) and MHC II is able to activate CD4$^+$ helper T cells and B cells (87).
Antibodies produced by B cells against viral proteins HA(88), NA(89), M2(90) and
NP(91) aid in viral clearance. T cells also play a major role in the IAV immune response.
CD8$^+$ cytotoxic T cells recognize and eliminate virus infected cells (92). To highlight
their importance, viral clearance is delayed if these cells are not present. Naïve CD4$^+$ T
cells can differentiate into T helper 1 cells (Th1) when a viral infection is detected.
These cells secrete cytokines (IFN-γ, Interleukin-2 (IL-2), and Tumor Necrosis Factor-α
(TNF- α), which enhance the activation of CD8$^+$ T cells and macrophage function and
also play a role in B cell differentiation (93). Other types of T cells are also involved.
Regulatory T cells (Tregs) promote a well-balanced viral immune response created by
CTL and CD4$^+$ T cells and also help with the resolution of inflammation (94). T helper
17 cells (Th17) counteract Tregs and enhance T helper cell viral responses (95). Overall,
the adaptive immune response is required for the resolution of infection and protection
from future infection, but it must be regulated appropriately.

Transcriptional Activation: PRRs and PAMPS. In addition to initiating an adaptive immune response, the pathogenic particles also trigger innate immunity. When PRRs present on epithelial and immune cells detect PAMPS or DAMPs created by the virus or the bacteria, an immune signaling cascade or activation of immune effector molecules is initiated (Figure 1A). Activation of PRRs during coinfection can induce inflammation through two mechanisms. The first is transcriptional activation of immune system genes. This starts by activating PRRs such as Toll-like receptors (TLRs), retinoic acid-inducible gene-I (RIG-I)-like receptors (RLRs), and certain Nucleotide oligomerization domain (NOD)-like receptors (NLRs). RLRs are cytoplasmic sensors that detect viruses. RIG-I is part of the RLR family and detects the 5′ triphosphate (PPP) of uncapped-RNA of IAV (96, 97). RIG-I deficiency has been linked to a delayed and attenuated antiviral response (98, 99). NLRs are another type of PRR. The NLRs have 22 members and are subdivided into four categories: NLRA, NLRB, NLRC, and NLRP (100). Nucleotide oligomerization domain-2 (NOD2) is an NLR part of the NLRC subfamily. It becomes activated by muramyl dipeptide (MDP) of bacterial peptidoglycan, hence it detects the peptidoglycan of *S. pneumoniae* (101, 102). Mice with NOD2 mutations have a higher susceptibility to bacterial and viral infections (103). TLRs are type I transmembrane proteins; there have been twelve murine and ten human TLRs characterized, but the most important ones when studying this coinfection are TLR2, TLR9, TLR3 and TLR7. TLR2 recognizes bacterial lipoprotein, lipoteichoic acids and lipomannans. TLR2 is important for recognizing PAMPs from gram-positive bacteria such as the peptidoglycan of *S. pneumoniae* (104, 105). *Tlr2*$^{-/-}$ mice have a difficult time clearing bacterial infection with *S. pneumoniae* primary infection, yet a difference in

immune response and bacterial outgrowth is not seen in post-influenza pneumococcal pneumonia (106-108). On the other hand, TLR9, which is embedded in an endosome membrane, recognizes 5'—C—phosphate—G—3' (CpG) deoxyribonucleic acid (DNA), present in *S. pneumoniae* (109). TLR3, also embedded in an endosome, detects viral double-stranded RNA, which is present in IAV (110). Deficiency in TLR3 in humans results in an increased risk of pneumonia, yet *Tlr3$^{-/-}$* mice appear to have improved mortality compared to wild-type mice due to a decrease in inflammation (111-113). TLR7 is also embedded in an endosome and recognizes single stranded RNA from IAV (114-116). *Tlr7$^{-/-}$* mice have delayed *S. pneumoniae* disease progression after IAV challenge due to decrease alveolar macrophage depletion, yet in the end, they still succumb to the coinfection (116). Importantly, this suggests that signaling through other immune receptors is important and that no single PRR may be responsible for inflammation during coinfection.

Transcriptional Activation: Downstream Adaptor Proteins. After receptor activation, downstream adaptor proteins become stimulated. The Mitochondrial antiviral-signaling protein (MAVS) becomes activated by RIG-I (Figure 1). Sun et al. explored the effect of *Mavs* deficiency in mice during viral infections, and found that these mice have difficulty fighting viral infections due to a reduction in interferon production (117). The Receptor-interacting serine/threonine-protein kinase 2 (RIPK2) adaptor protein becomes activated when it receives signals from NOD2. Lupfer et al. found that *Ripk2$^{-/-}$* mice are more susceptible to IAV infection due to defective induction of damaged induced degradation of the mitochondria (mitophagy). These mice also showed increased production of proinflammatory cytokines IL-18 and IFN-γ (118). Adaptor protein

Myeloid differentiation primary response gene 88 (MYD88) is an essential member of several signaling pathways responsible for proper immune function including TLRs and interleukin-1 family cytokine receptors. It has been previously shown that deficiency in *Myd88* leads to susceptibility to infection with pyogenic bacteria like *S. pneumoniae*. *In vivo*, mortality, morbidity, and bacterial growth in *Myd88* deficient mice were enhanced compared to WT mice (119, 120). In addition, mice lacking this protein cannot signal by using the IL-1R signaling pathways (121, 122). MYD88 protein is able to interact with almost all TLRs, except TLR3, which signals in a MYD88-independent pathway (123). TIR-domain-containing adapter-inducing interferon-β (TRIF) is another adaptor protein activated by some TLRs. It has been noted in murine studies that the TRIF/TLR3 pathway is responsible for excessive inflammation leading to pulmonary edema, increased proinflammatory responses and mortality (124).

Transcriptional Activation: Transcription Factors. MYD88 and/or TRIF can subsequently activate the transforming growth factor β-activated kinase (TAK1) (Figure 1 B). The kinase then connects with the inhibitor of κB (IκB) kinase kinases (IKK) complex which results in phosphorylation of IκB and the nuclear translocation of the transcription factors nuclear factor kappa-light-chain-enhancer of activated B cells (NF-κB) (125). NF-κB is a family of five transcription factors that are upstream regulated by adaptor proteins and PRRs (126). They can also be activated by oxidative stress and cytokines. Among this family of transcription factors, the dimer RelA (p65)/p50 is the most well-known. It resides in the cytoplasm of immune cells. The dimer is kept inactive by a family of IκBs (α/β/γ). For the p65/p50 dimer to become activated, the serine residues of the IκBs have to be phosphorylated by the IKK complex, which is triggered

by PRR-adaptor protein interaction. The phosphorylation of IκBs results in polyubiquitination (Lys^{21}/ Lys^{22}) and 26S proteasome degradation of IκBs resulting in nuclear translocation of the NF-κB dimers. Once in the nucleus, the dimers bind to the promoters of many genes through κB motif interactions. The dimer also initiates transcription of IκB genes as a negative feedback mechanism to prevent excessive inflammation (127). NF-κB is involved in many processes, hence, unregulated activation of it can lead to reduction of apoptosis, increased cell survival and increased inflammation. Although over activation of NF-κB would produce increased inflammation, which would results in an enhance immune response in the lung, enhanced inflammation only further impairs lung function and makes pneumonia worse.

In addition to NF-κB, other transcription factors like Interferon Stimulated gene factor 3 (ISGF3) and Interferon Regulatory Factor 3 or 7 (IRF3/7) play a role in coinfection pathogen recognition. TLR3 and RIG-I initiate a signaling cascade which results in the activation of IRF3/7. These transcription factors localize to the nucleus and initiate the transcription of Type I interferons (IFN-α/β). The interferons then signal the interferon-α/β receptors (IFNAR) in an autocrine/paracrine manner resulting in their activation (Figure 1C). After ligand recognition, the heterodimer interferon-α/β receptor (IFNAR) 1/2 couple with receptor-bound Janus kinases (JAK1) and tyrosine kinase 2 (Tyk2) (128). These kinases cross phosphorylate each other which results in their activation. Once activated, they phosphorylate tyrosine kinases leading to recruitment and phosphorylation of two latent proteins called Signal transducer and activator of transcription (STAT) 1/2. STAT 1/2 deficiency has been linked to increased susceptibility to IAV and other viruses (129, 130). STAT 1 and STAT 2 interact with

Tyk2 followed by activation of IRF9. The complex of STAT1/2 and IRF9 translocate to the nucleus and form the heterotrimeric transcription factor Interferon-stimulated gene factor 3 (ISGF3).

Transcriptional Activation: Cytokines. In the nucleus, NF-κB and ISGF3 initiate transcriptional regulation of immune signaling molecules called cytokines. IFN-α/β are cytokines that serve an important protective function against viral replication, yet they increase bacterial burden by decreasing neutrophil responses needed to fight off bacterial pathogens (131-134). Type 2 interferon, IFN-γ, production has also been linked to impaired alveolar macrophage function and bacterial burden after coinfection (73, 80, 135-137). Interleukin-6 (IL-6) and tumor necrosis factor-α (TNF-α) are proinflammatory pyrogenic cytokines transcribed by NF-κB (138). Interleukin-1-beta (IL-1β) is another proinflammatory pyrogen produced by leukocytes and is a key inflammatory mediator that can regulate the production of TNF-α and IL-6 (139-141). IL-1β plays an important role in both the innate and adaptive immune response and irregularities in this cytokine have been linked to inflammatory disorders, tumor angiogenesis and metastasis (142). It is synthesized as an inactive precursor (pro-IL-1β) that must be activated by a multiprotein complex called the inflammasome (143). NF-κB is also in charge of the transcriptional regulation of the components necessary to form the inflammasome (129, 144).

Inflammasome Activation. There are different types of inflammasomes, yet the two most important ones during this coinfection are the NLR Family Pyrin Domain Containing 3 (NLRP3) and Absent in melanoma 2 (AIM2) inflammasomes. The NLRP3 inflammasome is a multiprotein complex containing the NLRP3 protein, the apoptosis-

associated speck-like protein containing a caspase recruitment domain (ASC) and the cysteine protease caspase-1. NLRP3 senses dsRNA from IAV (145). It also senses DAMPs like reactive oxygen species, and K^+ and H^+ fluxes resulting from cell damage caused by IAV or *S. pneumoniae* infection (143, 146-149). AIM2 can also activate the inflammasome when it recognizes DNA in the cytoplasm from *S. pneumoniae* (148, 150). Active caspase-1 in the inflammasome cleaves inactive pro-IL-1β into their active forms and triggers pyroptotic cell death. Once activated, IL-1β leaves the cell through pores and activates inflammation (151-153). Pro-IL-1β can also become active by Fas signaling/Caspase-8 and by a noncanonical inflammasome pathway involving Caspase-11 or by extracellular cleavage by neutrophil protease 3 (154).

Pathogen Immune Evasion

Even though the immune system is complicated, pathogens such as IAV and *S. pneumoniae* have found a way to evade it.

Influenza A Virus. IAV has certain mechanisms to evade the immune system (155). NS1 inhibits the recognition of 5'-triphosphate (uncapped) viral ssRNA by innate receptors (156). It can also inhibit dendritic cell maturation (157). Overall, it has been shown that IAV can prevent monocytes from differentiating into dendritic cells by affecting antigen endocytosis and reducing the amount of CD11c, CD172a, CD1w2 and CCR5 cell surface proteins present (157). In addition, PB2 (158), PB1 (159) and PA (160) play a role in cap snatching, which limits innate immune receptors from recognizing IAV RNA and results in diminished immune signaling. IAV can also evade natural killer cells by replicating inside them and inducing apoptosis (161). IAV is able to

evade the humoral immune response due to antigenic variation, which can be categorized either as antigenic shift or drift. Antigenic drift occurs when the virus experiences small changes in its genome due to point mutations. During antigenic drift, mutations can accumulate preventing antibodies from recognizing the virus. Antigenic shift is the virus' ability to change HA and/or NA proteins. This allows the virus to have infinite subtypes. It occurs when the virus jumps from one reservoir to another creating an antigenically distinct virus. It can also occur through re-assortment, when two viruses infect one reservoir simultaneously also resulting in a distinct virus through genetic recombination (162). During antigenic shift, the emergence of antigenically unique viruses occurs. Hence, antibodies have no effect on the new virus, so it takes the body a long time to produce the proper immune response (163, 164). A final way IAV can evade the immune system is by interfering with T cell recognition. This occurs when amino acid variation and alteration of epitope regions interferes with antigenic presentation and detection (58). For example, mutations in the Cytotoxic T lymphocyte (CTL) epitopes and amino acid substitutions in the NP aid IAV to escape from CTLs (165).

S. pneumoniae. The innate immune system usually eliminates *S. pneumoniae* by opsonizing, phagocytizing and killing the bacteria. This is possible due to complement opsonizing the bacteria and neutrophil receptors interacting with the complement proteins. *S. pneumoniae* immune evasion targets this mechanism (166). Several structural components of *S. pneumoniae* aid it through immune evasion. Its polysaccharide capsule covers its cell wall and prevents most of the PAMPs in the cell wall from being detected by PRRS. This capsule is also antigenically diverse, thus preventing the production of a universal antibody against *S. pneumoniae*. The capsule also prevents the bacteria from

being phagocytosed by macrophages, and to be damaged by toxic substances produced by neutrophils. It also prevents the bacteria from getting trapped in the mucus in the lungs, and it impedes opsonization by complement (167). The production of proteins such as PspA by *S. pneumoniae* inhibit one of the complement pathways by competing with its attachment to the bacteria (168). PLY released from the bacteria also aids in immune evasion by shifting the focus of the complement proteins to the toxin and not to the bacterial itself (169). Finally, protein NanA also impedes complement deposition and disrupts neutrophil killing by deglycosylation of complement components (170). In addition to having its own protective mechanism, *S. pneumoniae* can benefit from IAV infecting the host.

   IAV Facilitates *S. pneumoniae* infection. IAV facilitates the adherence of *S. pneumoniae* to airway epithelium by damaging the epithelial layers. The damage results in exposure of the underlying basement membrane and impairment of progenitor epithelial cells impeding their repair. Damage results in exposure of receptors such as fibrin and the platelet activating factor receptor (PAFr) (171). The pneumococcal surface protein A (PsaP) and pneumococcal serine-rich repeat protein (PsrP) are then able to interact with these receptors. In addition to exposure of receptors, the neuraminidase protein of IAV desialylates terminal sialic acids exposing galactosyl moieties to serve as ligands for galectins. Galectin 1 and 3 can then bind to the bacteria's capsular polysaccharide increasing adherence to the lung tissue (172). IAV can also impede bacterial clearance (55, 73, 173-175). Pittet et al. compared bacterial clearance on the trachea of uninfected mice versus those infected with IAV. A decrease in bacterial clearance was seen on the mice infected with IAV. As previously stated, *S. pneumoniae*

resides in the nasal epithelium, and to reach the lungs it requires tracheal passage. IAV damages the cilia on the tracheal epithelium resulting in decreased tracheal mucocialiary velocity. This impedes the normal pneumococcal removal by movement of the mucus and ciliary beating and results in increased bacterial numbers that could eventually reach the lungs to cause pneumonia.

Finally, IAV infection enhances bacterial growth due to the depletion of alveolar macrophages (73, 135, 174, 176) and dysregulation of neutrophils (177-179). Following the coinfection, an elevated number of neutrophils is seen. Even though the quantity of these cells increases, their antimicrobial ability is reduced by the lack of activity from the myeloperoxidase enzyme stored in their azurophilic granules. This enzyme is involved in inflammation and oxidative stress (180). Thus, infection with IAV facilitates the invasion and inhibits the removal of *S. pneumoniae* leading to a severe infection, pneumonia, and even death.

Treatment

During coinfection, antiviral drugs can decrease complications from bacterial coinfections when given during the viral infection. This may prevent the initial tissue damage that aids *S. pneumoniae* superinfection (181). Previous studies show that treatment with β-lactam antibiotics, like ampicillin, can kill the bacteria but increase inflammation by the release of pneumococcal cell wall components through bacterial lysis (181). On the other hand, treatment with protein synthesis inhibitors that have a bacteriostatic effect, such as clindamycin, can improve the clearance of the bacteria without further stimulating the immune system via bacterial cell lysis (182). Although

specific cytokines play pathological roles during coinfection, the treatment of human patients with corticosteroids during coinfection provides no benefit (183-186). Thus, the global inhibition of inflammation may not be beneficial, and the specific roles of cytokines need to be examined to determine which have therapeutic potential. Thus, effective treatment of coinfection requires addressing the pathogens and immune-mediated pathology.

HYPOTHESES

Even though a vast amount of information is known about its regular biological function, the specific role played by IL-1β during the coinfection of IAV and *S. pneumoniae* has not been thoroughly studied. IL-1β plays a role in the activation of other pro-inflammatory cytokines such as TNF-α and IL-6 (141). These other cytokines are enhanced during this coinfection resulting in increased inflammation (171). Since TNF-α and IL-6 are enhanced during the coinfection then the production of IL-1β might be elevated as well. I propose the following two hypotheses to explain the production of IL-1β in this coinfection and the benefits that might result from its regulation:

Hypothesis one: IL-1β production will be enhanced during the coinfection of IAV and *S. pneumoniae in vitro* in bone marrow derived macrophages and *in vivo* in C57Bl/6 mice compared to its production during the single infection.

Hypothesis two: Controlling IL-1β's production in the C57Bl/6 mice by using neutralizing antibodies will help improve the immunopathology resulting from this coinfection.

METHODS

Overall Experimental Design

Experiments in cell culture and mice were performed to check their immune response to the coinfection of influenza A/PR/8/34 H1N1 virus and Type 3 *S. pneumoniae* (ATCC 6303). Cell cultures were single infected or coinfected with infectious virus and/or bacteria, and samples were collected to check cytokine and protein production as well as gene expression. Mice were infected and monitored for mortality and morbidity after being single infected or coinfected with virus and/or bacteria. In some experiments, lungs from infected mice were collected to check for cytokine production, immune cell infiltration and viral and bacterial titers.

Mice

Cell cultures of bone-marrow-derived-macrophages (BMDMs) were generated by harvesting bone marrow from tibia and femurs from WT, or *Nlrp3$^{-/-}$, Myd88$^{-/-}$, Aim2$^{-/-}$, Casp1$^{-/-}$, Asc$^{-/-}$, Tlr7$^{-/-}$ Tlr2$^{-/-}$,Ripk2$^{-/-}$, Trif$^{-/-}$,* and *Mavs$^{-/-}$* knockout mice all on the C57BL/6 genetic background. After bone marrow harvesting, cells were differentiated in L929 conditioned medium for 5 days as previously described (187). BMDMs were then counted and seeded in 12 well plates (Thermo Scientific, 130185) . The following day, BMDM were infected as described below.

Pathogen-free C57BL/6, *Nlrp3$^{-/-}$, Myd88$^{-/-}$, Aim2$^{-/-}$* mice (*Mus musculus),* were originally obtained from The Jackson Laboratory and then bread in-house. *Casp1$^{-/-}$, Asc$^{-/-}$, Tlr7$^{-/-}$,* and *Tlr2$^{-/-}$* knockout mice were housed at St. Jude Children's Research

Hospital and have been reported previously [39, 77, 78]. CO_2 asphyxiation followed by cervical dislocation was used to euthanize the mice. Infected mice were maintained in a Biosafety level 2 facility. All breeding and experiments were performed at the Missouri State University Vivarium in accordance with Institutional Animal Care and Use Committee (IACUC) guidelines under protocol (January 8, 2016; approval #16.009 and February 17, 2016; approval #16.015), the AVMA Guidelines on Euthanasia, NIH regulations (Guide for the Care and Use of Laboratory Animals), and the U.S. Animal Welfare Act of 1966.

Preparation of Viral and Bacterial Stocks

Viral and bacterial infectious agents were used in this study. Prior approval for this project was obtained from the Institutional Biosafety Committee (IBC) on October 2nd, 2015. Highly pathogenic mouse-adapted influenza A/PR/8/34 H1N1 virus hereafter referred as "PR8" stocks were propagated by allantoic inoculation of hen's eggs with seed virus. Embryonated chicken eggs were obtained from Charles River Labs and infected with IAV at 10 days old. Allantoic fluid was collected after three days. Plaque assays were performed using Madin-Darby canine kidney (MDCK) cells (a gift from Dr. Paul Thomas, St. Jude Children's Research Hospital) to determine stock titer. Two days before assay MDCK cells were seeded in 12-well plates in minimal essential medium (MEM) with 5% Fetal Bovine Serum (FBS) (GE Healthcare Life Sciences, SH30118.03), Penicillin/Streptomycin (Pen/Strep) (Corning, 30-002-Cl) and Glutamine (Lonza, 17-605E). Ten-fold viral dilutions were prepared in MEM without serum. Wells were washed twice with 1 ml of PBS. 100 µl of each virus dilution was added to each well.

Plates were incubated at 37°C/5%CO$_2$ for one hour. Overlay (2% agarose and 2x MEM/Bovine Serum Albumin (BSA) at 1:1 ratio) was prepared after 40 minutes of incubation. Following the one hour incubation period, the infection medium was removed and 2ml of overlay per well was added. Once agar hardened, plates were incubated upside down for 3 days at 37°C/5%CO$_2$. After 3 days, agar plugs were removed with a spatula and plaques were stained with 1% crystal violet. The stain was removed, the wells were washed and the plate dried upside down on a paper towel. Plaques were counted visually.

Type 3 *S. pneumoniae* (ATCC 6303) was used in our studies. Colony Forming Unit (CFU) assays were performed to confirm bacterial stock concentrations after growth of bacteria in Brain Heart Infusion (BHI) broth at 37°C/5%CO$_2$ overnight. Petri dishes (Fisher brand, FB0875712) were filled with 25ml of BHI (BD 237500) agar (Fisher Bioreagent BP1423-500) and were kept at room temperature until solidified. A ten-fold serial dilution (10^{-1} to 10^{-6}) was made with 900µl of BHI broth and 100µl of bacterial stock. Using a P200 micropipette, 100 microliters of each dilution was dispensed onto each plate (1 plate per dilution). Plates were incubated upside down at 37°C/5%CO$_2$. The following day, colonies were inspected and counted visually. The dilution with colonies in the 30 -300 range was selected to obtain the CFU/ml.

Infection schemes and Treatment

For *in vitro* studies, macrophages were washed 2X with phosphate buffered saline (PBS), and 200 µl of Roswell Park Memorial Institute (RPMI) medium (Corning,10-040e) was then added to each well. Multiplicity of infection (moi =#pathogens/#of cells)

was used to calculate the volume of pathogen stock to add (#of cells in well X MOI / concentration of pathogen stock). Macrophages were then mock infected, or single infected, either with 10 moi of PR8 or 1 moi of *S. pneumoniae*, or coinfected with 10 moi of PR8 then 3 hours later 1 moi of *S. pneumoniae.* After an additional hour, 200 μl RPMI with 20% FBS was added to all wells (Figure 2). Cell lysates and supernatants were then collected at 6, 12 or 24 hr time points for analysis by western blot, real-time quantitative polymerase chain reaction (qRT-PCR) or enzyme-linked immunosorbent assay (ELISA).

For *in vivo* studies, mice were anesthetized on day 0 by intraperitoneal injection with 80mg/kg Ketamine and 8mg/kg Xylazine diluted in PBS. Mice were infected with 125 PFU PR8 intranasally in a volume of 30 μl of PBS. Some mice were mock infected or coinfected on day 7 with 1000 CFU *S. pneumoniae* intranasally in a volume of 30 μl of PBS (171, 188). Additional mice were also singly infected with 1000 CFU *S. pneumoniae* on day 7. At all time points, mice were monitor at least daily for weight loss and mice were euthanized when they achieved 30% weight loss or became moribund. Alternatively, mice were euthanized on day 9 to collect lungs and blood for examining gross lung pathology, cytokine levels by ELISA, cell population by flow cytometry and for determining pathogen titer by CFU and PFU assays. Viral titers from homogenized lungs were analyzed by plaque assay using MDCK cells as previously reported (189). Quantification of *S. pneumoniae* from lung homogenates was done by making 10-fold serial dilutions of the lung homogenate and plating 100ml on brain heart infusion agar plates and incubating in a 37 ˚C incubator with 5% CO_2 for 24 hr (Figure 3).

Some groups of mice were treated after coinfection on day 7 by intraperitoneal injection with either clindamycin hydrochloride (60mg/kg), and/or an IL-1β neutralizing

antibody (Armenian Hamster IgG anti-mouse/rat IL-1β, 25 mg/kg), or an isotype control

antibody (Armenian Hamster IgG 25 mg/kg) (BioXcell, clones BE0246 and BE0091).

Clindamycin injections were given twice a day starting 18 hours after coinfection.

Antibody injections were started 1 hour after coinfection and administered every other

day. All experiments were performed at least in triplicate (Figure 4).

Sample Analysis

Enzyme-linked immunosorbent assay (sandwich ELISA) was used to analyze

cytokine levels in cell culture supernatants or whole lung homogenates were analyzed

using mouse Ready-SET-Go ELISA kits (eBioscience) for IL-1β (88-7013), IL-6 (88-

7064), or TNF-α (88-7324). Assays were performed using the manufactures

recommendations. Microtiter plates were read at 450 nm using a BioTek ELx800

microplate reader.

Protein expression was analyzed through Sodium Dodecyl Sulfate Polyacrylamide

Gel Electrophoresis (SDS-PAGE) (Fisher Bioreagens BP166-500) and Immunoblotting.

4x SDS loading dye (glycerol, bromophenol blue, 2-beta-mercaptoethanol, Tris buffer

and water) was added to lysates collected from *in vitro* infected BMDMs at different time

points as described above (*in vitro* infection scheme and collection). Lysates were boiled

at 95°C for 20 minutes, centrifuged for 5 seconds and subjected to SDS-PAGE at 100V

for two hours. Gels were electrophoretically transferred onto polyvinylidine difluoride

(PVDF) membranes (GE Healthcare life Sciences,10600023) at 40V for 45 minutes.

PVDF membranes were transferred to a container with 10 mls of 5% milk in Tris Buffer

Saline (Fisher Bioreagents, BP152-1) + 0.05% Tween 20 (Fisher Scientific, BP337-500)

(TBST) for blocking the membrane. The container was placed on a shaker at room temperature for one hour. Milk was discarded and 10 mls of protein specific primary antibodies diluted in 5% milk in TBST was added to the container (Table 1). The container was covered and kept under 4°C refrigeration overnight. The following day the diluted antibody was saved and the membranes were washed 3 times with 10 mls of TBST. Membranes were incubated at room temperature for 5 minutes on the shaker for every wash. After the last wash was discarded, protein specific secondary antibodies diluted in 5% milk was added to the container (Table 1). The container was placed on a shaker at room temperature for 45 minutes. After incubation, the diluted antibody was saved and the membranes were washed 4 times with 10 ml of TBST. Membranes were incubated at room temperature for 5 minutes on the shaker for every wash. The last wash was not discarded, instead the membranes were transferred to another container and were finally treated with SuperSignal West Femto Maximum Sensitivity Substrate (ThermoScientific 34096). Bands were visualized using Azure biosystems C300 imaging system.

Viral titers from homogenized lungs were analyzed by using MDCK cells through a plaque assay, detailed procedure can be found above (preparation of viral and bacterial stocks section). Plaque forming units were identify visually. Quantification of *S. pneumoniae* colony counts was done through CFU assay, detailed procedure can be found above (organism of interest section). Identification of colonies was done by visual inspection.

Flow Cytometry was used to analyzed cell population in *in vivo* experiments. Lungs were collected on day 9 post-infection. Lungs were homogenized by passing them

through a 70μm cell strainer using RPMI and the back of a syringe. Homogenate was centrifuged for 7 minutes at 400g, supernatant was removed, and pellet was resuspended in 5 mls of RBC lysis buffer and 5 ml RPMI. Samples were centrifuged for 7 minutes at 400 g. Supernatant was removed and pellet was resuspended in 5 mls of 37.5% percoll at room temperature and centrifuged for 20 minutes at 1000g. All but 500μl of percoll was removed and 2mls of PBS were added. Samples were centrifuged at 400 g for 7 minutes, supernatant was removed and samples were stained with fluorescent antibodies (Table 2). Samples were run on the flow cytometer. Data was analyzed using FCS Express. Material were obtained from Life Technologies.

Histopathology was used in this study to examine diseased mice lungs. C57Bl/6 and transgenic mice were euthanized on day 9, two days after coinfection, to collect their lungs. Uninfected lungs from two mice were obtained at the same time as controls. Lungs were kept in formalin buffer. Fixed lungs were placed in individual cassettes and were processed in a Leica tissue processor on a 10-hour run to make cells transparent and able to be stained. Each cassette containing the processed tissue was then embedded in a block of paraffin. A Leica microtome StatLab low profile blades was used to cut the blocks. These were then placed onto Apex charged slides, usually with 2 or more sections per slide. Slides were then stained with hematoxylin and eosin. Permount toluene-based mounting media was used to cover slip the slides. Slides were examined by pathologist Dr.Gilbert. Each lung was scored using a system based on 27 characteristics (Table 3). Slides were imaged on an Olympus C23 microscope with an Amscope 5 mega-pixel digital microscope camera.

Real-time qPCR was used in this study to detect the expression of different cytokine genes. Extraction of total mRNA was done by using TRIZOL (Invitrogen,AM97381). mRNA was then reverse-transcribed into cDNA using a high capacity cDNA reverse transcription kit (Applied Biosystems, 4368814). cDNA samples were analyzed by real-time quantitative PCR (RT-qPCR) using DyNAmo HS SYBR Green qPCR Kits (Thermo Scientific, F,410L) and relative values normalized to β-actin control (see Table 4 for primer sequences).

Statistical Analysis

For *in vitro* experiments and *in vivo* cytokine production, one-way ANOVA with Tukey's post hoc analysis was performed using PRISM6. For weight loss during *in vivo* experiments, two-way ANOVA with Dunnett's post hoc analysis was performed using PRISM6. For survival *in vivo* experiments, survival analysis was performed using the Wilcoxon test using PRISM6. For the histological score, a one-way ANOVA with the Kruskal-Wallis test was performed. A p value <0.05 was considered statistically significant for all tests.

RESULTS

To determine mechanisms by which the coinfection of IAV and *S. pneumoniae* affect IL-1β and other cytokines, bone marrow derived macrophages (BMDM) were infected with influenza A/PR/8/34 H1N1 (PR8) and *S. pneumoniae* ATCC 6303 type 3 strain (*S.p.*) either alone or 3 h apart (See Figure 2 for infection scheme).

Increased Production of Cytokine *in vitro* During Coinfection

Cytokine levels in culture supernatants were compared to uninfected controls after 24 h. A significant increase in the level of IL-1β was seen during coinfection of IAV and *S.p.* compared to untreated or single infected samples (Figure 5A). Significant increases in the production of IL-6, and TNF-α in coinfected samples were also observed (Figure 5 B-D).

Enhanced Production of IL-1β can Result from Bacterial Overgrowth.

Previous reports show that IAV and *S.p.* coinfection results in increased bacterial growth (73, 135, 171, 190). To determine if *S.p.* growth affects cytokine production during coinfection *in vitro*, BMDMs were infected with PR8 and then live or heat-killed *S.p.* was added to wells either alone or 3 h apart from PR8. The heat-killed bacteria should only be able to initially activate PRRs by peptidoglycan detection, yet since it is dead, additional bacterial growth should not occur. Testing different amounts of bacteria could have been another way to examine the effect of bacterial numbers on IL-1β levels, yet since we were not interested in the specific amount required for IL-1β production, we did not go this path. Samples collected after 24 h indicate the production of IL-1β, TNF-α and IL-6 levels were impacted negatively by heat killing the bacteria. However, even when

macrophages were coinfected with PR8 and heat killed *S.p.*, there was still an increase in IL-1β over single infections alone. Thus, bacterial overgrowth can only partially be responsible for enhance cytokine production (Figure 6 A-C).

Overproduction of IL-1β is not Associated with Enhanced Inflammasome Activation. IL-1β is produced as an inactive precursor that must be cleaved to be functionally active. Enhanced IL-1β observed during coinfection could, therefore, result from increased expression of pro- IL-1β or from the enhanced activation of IL-1β by caspase-1 in the inflammasome. Inflammasome activation was first examined by generating BMDM from WT mice or mice deficient in inflammasome components $Asc^{-/-}$, $Casp1^{-/-}$, $Nlrp3^{-/-}$ or $Aim2^{-/-}$. Macrophages were then infected with PR8 and *S.p.* singly or coinfected 3 hours apart. In cells lacking the inflammasome components caspase-1, ASC, or NLRP3, it was observed through ELISA that IL-1β levels significantly decreased compared to WT (Figure 7A). However, BMDM deficient in AIM2 did not show a significant difference compared to WT cells (Figure 7A). The inflammasome is clearly required for pro-IL-1β activation during single infections or coinfection, but it is not clear if there is enhanced Caspase-1 activation in coinfections. To answer this question, the same infection scheme was used and western blots were performed to check for caspase-1 activation. However, active caspase-1 (caspase-1 p20) levels were similar regardless of whether BMDM were singly infected or coinfected (Figure 7B). This suggests that enhance IL-1β is not due to more pro-IL-1β being activated by caspase-1.

Overproduction of Pro-IL-1β is Associated with Enhanced NF-κB Activation. As enhanced Caspase-1 activation which would result in more pro- IL-1β being cleaved is not evident during coinfection, we examined pro-IL-1β expression to determine if

increased signaling through PRRs during coinfection enhances the activation of signals

that will initiate the production of pro-IL-1 β. BMDMs were infected with PR8 and *S.p.*

alone or coinfected 3 h apart. Samples were collected at 6, 12 or 24 h after initial

infection and examined by western blot for pro-IL-1β expression. It was observed that

pro-IL-1β expression was enhanced during coinfection more than singly infected samples

(Figure 8A). The transcription factor NF-κB initiates transcription of the gene responsible

for production of pro-IL-1β (191, 192). To verify that NF-κB is important during

coinfection, BMDMs were infected and samples collected at 6, 12, and 24 h after initial

infection. Western blots of phosphorylated-IκBα (p-IκBα) and total IκBα were performed

to determine activation of the NF-κB pathway. In agreement with increased pro-IL-1β

expression, p-IκBα levels were higher during coinfection, indicating enhanced NF-κB

activation, which would results in the elevated production of pro-IL-1β (Figure 8 A).

Finally, RNA was isolated from singly and coinfected BMDM at 6, 12, and 24 h after

initial infection and performed qRT-PCR. It was observed that IL-1β, TNF-α and IL-6

mRNA were all expressed at higher levels in coinfected samples (Figure 8 B-D).

Examination of Signaling Pathways Necessary for IL-1β Production *in vitro*.
As enhanced NF-κB activation appears to be responsible for more IL-1β, we next

examined the signaling pathways upstream of NF-κB (Figure 1). Various TLRs, NLRs

and RLRs can facilitate NF-κB activation through adaptor proteins. I hypothesized that

during coinfection, the NOD2-RIPK2 pathway could respond to *S.p.* peptidoglycan

fragment muramyl di-peptide (MDP), RIG-I-MAVS pathways would respond to IAV

RNA, and TLRs 2, 3, 7 and 9 could respond to their various ligands and activate TRIF or

MYD88. Each of these pathways has the potential to activate NF-κB and subsequently

enhance pro-IL-1β expression. Thus to determine the pathways involved in pro-IL-1β expression during coinfection, BMDMs deficient in *Ripk2*^{-/-}, *Trif*[/-], *Myd88*^{-/-} or *Mavs*^{-/-} were infected and the effect on IL-1β production in culture supernatants 24 hours after initial infection was examined. It was observed that only coinfected *Myd88*^{-/-} BMDM had significantly reduced IL-1β compared to WT BMDM (Figure 9A). BMDM from *Tlr2*^{-/-} or *Tlr7*^{-/-} mice were then examined, and it was found that only *Tlr2*^{-/-} BMDM had significantly impaired IL-1β production during coinfection compared to WT cells (Figure 9B). As the TLR2-MYD88 signaling axis was most responsible for the increased expression of IL-1β, RNA from singly and coinfected BMDM obtained from WT mice at 6, 12, and 24 h after initial infection was isolated and qRT-PCR was performed. Interestingly, infected cells with either IAV, *S.p.* or coinfected showed enhanced expression of MYD88 (Figure 9C). Thus, it was hypothesized that MYD88 was important because at the time of coinfection, after 3 hours of initial IAV stimulation, there was more MYD88 available for *S.p.* to activate and potentiate a signal. To further examine this enhanced signaling capacity during coinfection, BMDMs were infected with the same amount of the ligand peptidoglycan (PGN) either at the same time as IAV or 3 hours apart like previously performed with *S.p.;* elevated levels of IL-1β were seen when the second signal was given after 3 hours of initial IAV infection (Figure 9D). Thus, time in between the coinfection results in an increase of IL-1β likely due to more MYD88 being available for signaling.

Pathways Regulating IL-1β *in vivo* During Coinfection

We next examined the effects of coinfection *in vivo* on cytokine production and inflammation. Mice were infected with a non-lethal dose of 125 PFU of PR8 intranasally on day 0 and then mock infected or coinfected with a non-lethal dose of 1000 CFU *S.p.* intranasally on day 7. Another group of mice were singly infected with *S.p.* on day 7. On day 9 after the initial flu infection (day 2 post-coinfection or *S.p.* infection), mice were euthanized and lungs were collected for further analysis. Similar to infection in BMDM, lungs from coinfected mice showed increased production of IL-1β, TNF-α and IL-6 during coinfection in WT mice compared to PR8 or *S.p.* single infection (Figure 10 A-C). Mice deficient in either *Nlrp3 or Myd88* showed significantly decreased production of IL-1β and *Myd88*^{-/-} mice also showed significantly lower TNF-α levels compared to WT coinfected mice. Intriguingly, no significant differences were seen in IL-6 levels in any of the transgenic mice compared to WT mice (Figure 10 A-C).

Morbidity and Mortality. To determine the effects of cytokine production dependent on NLRP3 and MYD88 on morbidity and mortality during coinfection, mice were infected as before and monitored for survival until day 14 after initial PR8 infection (day 7 post-coinfection). Although all genotypes of mice lost weight during infection with PR8, *Myd88*^{-/-} mice consistently exhibited the highest weight loss (Figure 11 A). As previously reported, *Aim2*^{-/-} mice lost significantly less weight during PR8 infection (Figure 11A) (193). However, no mice succumbed to PR8 infection alone due to the low infectious dose. Single infection with *S.p.* had little effect on weight loss due to the low infectious dose (Figure 11C). However, significant mortality was observed in *Myd88*^{-/-} mice infected *with S.p.* alone (Figures 11D). During coinfection, *Myd88*^{-/-} mice were more susceptible than WT mice (Figure 11 E-F). *Aim2*^{-/-} mice displayed a similar

morbidity and mortality (Figure 11E-F). Finally, although *Nlrp3*^{-/-} mice had similar

mortality compared WT mice, they recovered weight faster than any other genotype of

mice (Figure 11E-F).

  Lung Pathology and Viral and Bacterial Titers. To understand the accelerated

weight gain seen in *Nlrp3*^{-/-} mice, we further examined lung pathology and viral and

bacterial titers during coinfection. By day 9 (day 2 post-coinfection) PR8 was almost

completely cleared from the lungs of WT, *Myd88*^{-/-}, *Nlrp3*^{-/-} and *Aim2*^{-/-} mice and we

observed no significant differences in viral titers (Figure 12A). *S.p.* titers were still high

on day 9 (day 2 post-coinfection), but there was also no significant difference among the

WT and the *Myd88*^{-/-}, *Nlrp3*^{-/-} and *Aim2*^{-/-} mice. The bacterial titers in the lungs of *Myd88*^{-/-}

mice were non-significantly higher than the *Nlrp3*^{-/-} mice (Figure 12B). Bacterial titers

in the blood of coinfected mice euthanized on day 9 were also collected, and *Myd88*^{-/-}

mice had less bacterial titers present in the blood. Histopathology examination showed

that *Myd88*^{-/-} mice had less lung damage during coinfection than WT mice, yet when total

histological scores were compared among the genotype groups, no significance was

found (Figure 13 A-B). I thus conclude that decreased activation of the NLRP3

inflammasome, improves recovery from coinfection, perhaps by improving bacterial

clearance or by improving malaise. In contrast, *Myd88*^{-/-} mice have higher bacterial titers

in the lungs compared to the *Nlrp3*^{-/-} mice, which could explain why these mice succumb

to the infection. The lower bacterial titers in the blood of *Myd88*^{-/-} mice may also suggest

the dissemination of bacteria to other organs at an earlier time after coinfection. Though

this remains to be determined.

Immune Cell Infiltration into the Lungs During Single or Coinfection. To have a further understanding of the underlying mechanism behind the increased amount of IL-1β *in vivo* during coinfection, the immune cell populations during the different infection schemes were analyzed through flow cytometry. Macrophage, neutrophil, dendritic cells and lymphocytes populations were analyzed in WT and knockout mouse lungs, either single or coinfected, collected on day 9 (day 2 post-coinfection). A significant increase of neutrophils was seen in the *Myd88* deficient mice compared to WT (Figure 14A). A significant increase was also seen in the CD4 and CD8 populations in the *Myd88* deficient mice compared to WT (Figure 14B). However, these findings do not agree with the histology reports where infiltrates of neutrophils and lymphocytes were lower in the *Myd88* deficient mice, yet the difference between WT and *Myd88* deficient mice was not significant in the histology samples (Figure 13B). As yet, it is not clear why there is a discrepancy between the histology and flow cytometry sampling methods.

Effects of Individual or Combination Treatment with IL-1β Neutralizing Antibody and Clindamycin in Mice

To address the therapeutic potential of inhibiting IL-1β, WT mice were infected and treated them with an IL-1β neutralizing antibody beginning 1 h after coinfection. It was also considered that dramatic neutralization of IL-1β alone could impact viral or bacterial clearance. Thus, additional mice were treated with clindamycin or a combination of IL-1β neutralizing antibody and clindamycin, where clindamycin treatment was initiated 12 h post-coinfection. As a control, a fourth group of mice was injected with an Armenian Hamster IgG antibody isotype control (mock treatment). All

mice were then either monitored for 7 d for weight loss and survival or their lungs were collected on day 9 (2 d post-coinfection) to check cytokine levels and viral and bacterial titers in the lungs (see Figure 4 for timeline). The IL-1β neutralizing antibody, the clindamycin, and the combination of both treatments significantly decreased the levels of IL-1β present in the lungs during coinfection (Figure 15 A). The levels of IL-6 were also reduced, but the levels of TNF-α in the lungs were not (Figure 15 B-C). Treatment with clindamycin alone significantly improved mortality but not weight loss (Figure 16A-B). Treatment with IL-1β neutralizing antibody alone resulted in improved weight loss, but no difference in mortality compared to mock treated mice (Figure 16 A-B). Importantly, combination treatment with clindamycin and IL-1β neutralizing antibody resulted in improved weight loss and mortality (Figure 16A-B). To better understand these findings, the viral and bacterial titers in the lungs of mice on day 2 post-coinfection were also examined. There were no significant differences in viral titers between mock, the clindamycin, IL-1β neutralizing antibody, and the combination treatment groups (Figure 16C). It was found that clindamycin treatment significantly decreased bacterial numbers, but IL-1β neutralizing antibody did not significantly affect bacterial numbers (Figure 16D). No significant difference was found in the blood of coinfected mice among the treatment groups (Figure 16 E). To have a further understanding of the underlying mechanism behind the effects on morbidity and mortality among the different treatments lung histopathology and the cell population during the different drug treatments in coinfected WT mice was analyzed through hematoxylin & eosin (H&E) staining and flow cytometry. No significant difference among the treatments and the histological characteristic was observed (Figure 17A-B). No significant difference among the

treatment and the cell population was detected (Figure 18A-B). I thus conclude that combination treatment with IL-1β neutralizing antibody and clindamycin does not intervene with cell population or histopathology, at least at the time point we examined (Day 9). Combination treatment does have therapeutic benefit by inhibiting bacterial growth and preventing overt cytokine production resulting in improved morbidity and mortality associated with coinfections.

DISCUSSION

Inflammation allows a host to fight infection by facilitating the production, activation, and transportation of cytokines, receptors, and inflammatory cells. When improperly regulated or overly activated, inflammation can have detrimental results. The coinfection of IAV and *S. pneumoniae* has been linked to increased death rates during pandemic outbreaks, such as the 1918 "Spanish Flu", where pneumococcus was found in samples collected from infected individuals (9-12). Coinfections also occur during seasonal influenza epidemics to varying degrees (186, 194). Previous reports show that pro-inflammatory cytokines, such as TNF-α, IL-6, and type I interferons increase during coinfection; some displaying a detrimental effect and others a protective effect (131, 195). Thus, an improved understanding of the role for various cytokines and immune cells during coinfection is needed to understand how to treat this disease.

The role for IL-1β and the function of various inflammasomes in activating IL-1β have been examined in infectious disease susceptibility, inflammatory disorders, and cancer progression (196-199). However, the specific role played by IL-1β and the inflammasome during the coinfection of IAV and *S. pneumoniae* has not previously been studied. Through *in vivo* and *in vitro* experimentation using bone marrow derived macrophages and transgenic mice, I have examined the importance of IL-1β in this setting. To this end, I have examined both the host response to the pathogen as well as the effect of pathogen growth on IL-1β production (Figure 19). One possible explanation for more IL-1β is that coinfection results in an outgrowth of *S. pneumoniae*. However, our findings show that increased IL-1β levels during coinfection occur even if heat killed bacteria is used in combination with IAV. If dead bacteria in combination with IAV can

still cause enhanced IL-1β production, then bacterial outgrowth cannot fully explain the increased IL-1β observed during coinfection. Instead, this augmentation of IL-1β results from the overproduction of the precursor of IL-1β (pro-IL-1β), and overactivation of the transcription factor NF-κB by upstream pattern recognition receptors and the adaptor protein MYD88. Importantly, the initial infection of cells with IAV enhanced the expression of MYD88, which is associated with a stronger signal during the secondary bacterial infection with *S. pneumoniae*. Furthermore, we show that the NLRP3 inflammasome is important for the activation of IL-1β, but inflammasome activation itself is not elevated during coinfection. My data also implicate other inflammasomes or pathways involved in IL-1β production *in vivo*, as *Nlrp3* deletion only partially affected IL-1β production. One likely hypothesis is that a combination of NLRP3 and AIM2 contributes to inflammasome activation *in vivo*. Although *Nlrp3$^{-/-}$* mice had only a partial decrease in IL-1β levels, I did observe improved weight loss in these mice compared to WT mice that survived infection. To elucidate why these mice regain their weight, bacterial titers were analyzed. After 48 hours of a coinfection with a type 3 *S. pneumoniae* strain, the bacterial load in the lungs and blood of *Nlrp3$^{-/-}$* mice decreased compared to WT mice, yet they were not significantly different. Previous studies with *Nlrp3$^{-/-}$* mice single infected with 5 x 10^4 CFU of serotype 3 *S. pneumoniae* strain (6303) showed that six hours after infection bacterial numbers increased compared to WT, yet after 24 and 48 hours that bacterial load decreased improving morbidity. In WT mice after 24 and 48 hours, the bacteria disseminated to the blood and other organs such as the spleen, but not in *Nlrp3$^{-/-}$* mice (119). On my experiment on day 9, all the genotypes started gaining weight back. On day 12 the *Nlrp3$^{-/-}$* mice begun to gain more weight than

the WT, this could be due to the bacteria going back to normal levels resulting in a decrease in activation of pro-IL-1β by the AIM2 inflammasome. This trend is not seen in the *Aim2*^{-/-} mice 48 hrs after infection probably due to the activation of the NLRP3 inflammasome by the accumulation of damage already created until that point from the coinfection. This would also explain why elevated levels of IL-1β are seen in *the Aim2*^{-/-} mice. Overall, these data show that 48 hours after coinfection, enhanced IL-1β is responsible for prolonged or overt inflammation but does not significantly affect pathogen burden.

Although *Myd88*^{-/-} mice displayed decreased levels of IL-1β, this adaptor protein is involved in a variety of signaling pathways including most TLRs and the IL-1 receptor family. Therefore, *Myd88*-deficient mice are severely immunocompromised and, when coinfected, demonstrate increased mortality due to systemic complications (200). *Myd88*-deficient mice also show a non-significant difference of increased bacterial titers in the lung compared to *Nlrp3*^{-/-} mice and a significantly different decrease in the bacterial titers present in the blood. This suggest that bacterial burden in the lungs could be one reason why the *Myd88*^{-/-} mice show increase mortality. Although nonsignificant, the *Myd88*-deficient mice had a trend toward less lung damage compared to WT and the other genotypes. This could be due to decreased transcriptional activation, since most of the TLRs signal through MYD88, resulting in less production of pro-IL1β, less Caspase-1 activation and less cell death. These mice also showed an increase of IL-6 which can have an anti-inflammatory role in the immune system, this could cause the pro-inflammatory immune response against the bacteria not to begin on time after the co-infection resulting in increased mortality. This increase could also suggest that other anti-

inflammatory cytokines such as IL-10, which is known to act through MYD88-dependent signaling pathways (201), could be playing a role. In addition, the *Myd88^{-/-}* mice showed an increase in neutrophils, CD4 T cells and CD8 T cells. The reason for this is not clear, but perhaps less immune signaling during IAV infections means that the immune response to *S. pneumoniae* can proceed more normally. However, this is only speculation and needs further examination. The neutrophils present could also not be functioning correctly, be undergoing apoptosis or still be immature. A variety of subsets of T cells could be categorized as CD4 T cells and some of these subsets could be playing a role in the decrease survival of the *Myd88^{-/-}* mice, but this would again require further evaluation. Some of these subsets might also be present but not active. It has been shown that IAV induces IL-10 production, which can inhibit the activation of a type of cell called an invariant natural killer cells (iNKT) which usually have protective effects against this coinfection yet can produce lung damage. Mice missing these cells have increased mortality around 48 hours after coinfection (202). My findings agree with previous reports that *Myd88*-deficiency does not protect mice infected with the type 3 strain of *S. pneumoniae* (119). Overall, my findings suggest that a tightly regulated, not excessive, but sufficient amount of inflammation is necessary to have a proper immune response against this coinfection.

After understanding the importance of IL-1β during this coinfection, its therapeutic relevance in mice was studied. In the clinical setting, patients are usually treated with an antiviral, an antibiotic or steroid. Several studies report that steroid treatment does not improve morbidity and mortality during coinfection in human patients (183, 184). Beta-lactam antibiotics increase inflammation by releasing more bacterial ligands, potentially

worsening the condition in severe cases (182). Antivirals may improve survival in mice, particularly when combined with an antibiotic (135, 181, 203). The antibiotic clindamycin, which inhibits bacterial growth and reduces inflammation as a secondary effect, increases survival rates in mice during coinfection (135, 182). As I explored treatment options for coinfection, I used clindamycin in combination with IL-1β neutralizing antibody. Mice treated with IL-1β neutralizing antibody alone in my experiments showed improved weight loss, but this treatment alone did not improve overall survival. Treating the bacterial infection by using clindamycin and further controlling inflammation with the IL-1β neutralizing antibody in my experiments resulted in decreased weight loss and improved mortality in mice. Thus, IL-1β neutralization may have a place as an adjunct treatment to improve recovery time in cases of influenza A virus and *S. pneumoniae* coinfection.

REFERENCES

1. Pasman L. 2012. The complication of coinfection. Yale J Biol Med 85:127-32.

2. Seki M, Kosai K, Yanagihara K, Higashiyama Y, Kurihara S, Izumikawa K, Miyazaki Y, Hirakata Y, Tashiro T, Kohno S. 2007. Disease severity in patients with simultaneous influenza and bacterial pneumonia. Intern Med 46:953-8.

3. Dawood FS, Chaves SS, Perez A, Reingold A, Meek J, Farley MM, Ryan P, Lynfield R, Morin C, Baumbach J, Bennett NM, Zansky S, Thomas A, Lindegren ML, Schaffner W, Finelli L, Emerging Infections Program N. 2014. Complications and associated bacterial coinfections among children hospitalized with seasonal or pandemic influenza, United States, 2003-2010. J Infect Dis 209:686-94.

4. O'Brien KL, Walters MI, Sellman J, Quinlisk P, Regnery H, Schwartz B, Dowell SF. 2000. Severe pneumococcal pneumonia in previously healthy children: the role of preceding influenza infection. Clin Infect Dis 30:784-9.

5. Center for Disease Control and Prevention National Center for Health Statistics C. March 17, 2017 2017. Leading Causes of Death. Accessed 3/27.

6. Morens DM, Fauci AS. 2007. The 1918 Influenza Pandemic: Insights for the 21st Century. J Infect Dis 195:1018-1028.

7. Reid AH, Fanning TG, Hultin JV, Taubenberger JK. 1999. Origin and evolution of the 1918 "Spanish" influenza virus hemagglutinin gene, p 1651-6, Proc Natl Acad Sci U S A, vol 96.

8. McAuley JL, Hornung F, Boyd KL, Smith AM, McKeon R, Bennink J, Yewdell JW, McCullers JA. 2007. Expression of the 1918 influenza A virus PB1-F2 enhances the pathogenesis of viral and secondary bacterial pneumonia. Cell Host Micro 2:240-9.

9. McGuire LW, Redden WR. 1918. The Use of Convalescent Human Serum in Influenza Pneumonia-a Preliminary Report. Am J Public Health (N Y) 8:741-4.

10.   Soper GA. 1918. The Influenza Pneumonia Pandemic in the American Army Camps during September and October. 1918. Science 48:451-6.

11.   Brundage JF, Shanks GD. 2008. Deaths from bacterial pneumonia during 1918-19 influenza pandemic. Emerg Infect Dis 14:1193-9.

12.   Morens DM, Taubenberger JK, Fauci AS. 2008. Predominant role of bacterial pneumonia as a cause of death in pandemic influenza: implications for pandemic influenza preparedness. J Infect Dis 198:962-70.

13.   Palacios G, Hornig M, Cisterna D, Savji N, Bussetti AV, Kapoor V, Hui J, Tokarz R, Briese T, Baumeister E, Lipkin WI. 2009. Streptococcus pneumoniae coinfection is correlated with the severity of H1N1 pandemic influenza. PLoS One 4:e8540.

14.   Rice TW, Rubinson L, Uyeki TM, Vaughn FL, John BB, Miller RR, 3rd, Higgs E, Randolph AG, Smoot BE, Thompson BT, Network NA. 2012. Critical illness from 2009 pandemic influenza A virus and bacterial coinfection in the United States. Crit Care Med 40:1487-98.

15.   Palese P, Shah M. 2007. Orthomyxoviridae: the viruses and their replication. , 5 ed. Williams & Wilkins, Philadelphia.

16.   Bouvier NM, Palese P. 2008. The biology of influenza viruses. Vaccine 26 Suppl 4:D49-53.

17.   Palese P. 1977. The genes of influenza virus. Cell 10:1-10.

18.   Lu X, Shi Y, Gao F, Xiao H, Wang M, Qi J, Gao GF. 2012. Insights into avian influenza virus pathogenicity: the hemagglutinin precursor HA0 of subtype H16 has an alpha-helix structure in its cleavage site with inefficient HA1/HA2 cleavage. J Virol 86:12861-70.

19.   Lamb RA, Lai CJ, Choppin PW. 1981. Sequences of mRNAs derived from genome RNA segment 7 of influenza virus: colinear and interrupted mRNAs code for overlapping proteins. Proc Natl Acad Sci U S A 78:4170-4.

20.   Ye Q, Krug RM, Tao YJ. 2006. The mechanism by which influenza A virus nucleoprotein forms oligomers and binds RNA. Nature 444:1078-82.

21.   Area E, Martin-Benito J, Gastaminza P, Torreira E, Valpuesta JM, Carrascosa JL, Ortin J. 2004. 3D structure of the influenza virus polymerase complex: localization of subunit domains. Proc Natl Acad Sci U S A 101:308-13.

22.   Detjen BM, St Angelo C, Katze MG, Krug RM. 1987. The three influenza virus polymerase (P) proteins not associated with viral nucleocapsids in the infected cell are in the form of a complex. J Virol 61:16-22.

23.   Liu J, Lynch PA, Chien CY, Montelione GT, Krug RM, Berman HM. 1997. Crystal structure of the unique RNA-binding domain of the influenza virus NS1 protein. Nat Struct Biol 4:896-9.

24.   Lamb RA, Lai CJ. 1980. Sequence of interrupted and uninterrupted mRNAs and cloned DNA coding for the two overlapping nonstructural proteins of influenza virus. Cell 21:475-85.

25.   Richardson JC, Akkina RK. 1991. NS2 protein of influenza virus is found in purified virus and phosphorylated in infected cells. Arch Virol 116:69-80.

26.   Jagger BW, Wise HM, Kash JC, Walters KA, Wills NM, Xiao YL, Dunfee RL, Schwartzman LM, Ozinsky A, Bell GL, Dalton RM, Lo A, Efstathiou S, Atkins JF, Firth AE, Taubenberger JK, Digard P. 2012. An overlapping protein-coding region in influenza A virus segment 3 modulates the host response. Science 337:199-204.

27.   Chen W, Calvo PA, Malide D, Gibbs J, Schubert U, Bacik I, Basta S, O'Neill R, Schickli J, Palese P, Henklein P, Bennink JR, Yewdell JW. 2001. A novel influenza A virus mitochondrial protein that induces cell death. Nat Med 7:1306-12.

28.   Francis T, Jr. 1940. A New Type of Virus from Epidemic Influenza. Science 92:405-8.

29.   Dykes AC, Cherry JD, Nolan CE. 1980. A clinical, epidemiologic, serologic, and virologic study of influenza C virus infection. Arch Intern Med 140:1295-8.

30.   Hause BM, Ducatez M, Collin EA, Ran Z, Liu R, Sheng Z, Armien A, Kaplan B, Chakravarty S, Hoppe AD, Webby RJ, Simonson RR, Li F. 2013. Isolation of a novel swine influenza virus from Oklahoma in 2011 which is distantly related to human influenza C viruses. PLoS Pathog 9:e1003176.

31. Kimura H, Abiko C, Peng G, Muraki Y, Sugawara K, Hongo S, Kitame F, Mizuta K, Numazaki Y, Suzuki H, Nakamura K. 1997. Interspecies transmission of influenza C virus between humans and pigs. Virus Res 48:71-9.

32. Yassine HM, Lee CW, Gourapura R, Saif YM. 2010. Interspecies and intraspecies transmission of influenza A viruses: viral, host and environmental factors. Anim Health Res Rev 11:53-72.

33. Ran Z, Shen H, Lang Y, Kolb EA, Turan N, Zhu L, Ma J, Bawa B, Liu Q, Liu H, Quast M, Sexton G, Krammer F, Hause BM, Christopher-Hennings J, Nelson EA, Richt J, Li F, Ma W. 2015. Domestic Pigs Are Susceptible to Infection with Influenza B Viruses. Journal of Virology 89:4818-4826.

34. Smith W, Andrewes CH, Laidlaw PP. 1933. A Virus Obtained from Influenza Patients. The Lancet 222:66-68.

35. Saunders-Hastings PR, Krewski D. 2016. Reviewing the History of Pandemic Influenza: Understanding Patterns of Emergence and Transmission. Pathogens 5.

36. Neumann G, Kawaoka Y. 2015. Transmission of influenza A viruses. Virology 479-480:234-46.

37. Vries E, Tscherne D, Wienholts M, Cobos-Jiménez V. 2017. Dissection of the Influenza A Virus Endocytic Routes Reveals Macropinocytosis as an Alternative Entry Pathway. PLOS pathogens 7.

38. Matlin KS, Reggio H, Helenius A, Simons K. 1981. Infectious entry pathway of influenza virus in a canine kidney cell line. J Cell Biol 91:601-13.

39. Bui M, Whittaker G, Helenius A. 1996. Effect of M1 protein and low pH on nuclear transport of influenza virus ribonucleoproteins. J Virol 70:8391-401.

40. Martin K, Helenius A. 1991. Transport of incoming influenza virus nucleocapsids into the nucleus. J Virol 65:232-44.

41. Boivin S, Cusack S, Ruigrok RW, Hart DJ. 2010. Influenza A virus polymerase: structural insights into replication and host adaptation mechanisms. J Biol Chem 285:28411-7.

42. Te Velthuis AJ, Fodor E. 2016. Influenza virus RNA polymerase: insights into the mechanisms of viral RNA synthesis. Nat Rev Microbiol 14:479-93.

43. Shapiro GI, Krug RM. 1988. Influenza virus RNA replication in vitro: synthesis of viral template RNAs and virion RNAs in the absence of an added primer. J Virol 62:2285-90.

44. Plotch SJ, Bouloy M, Ulmanen I, Krug RM. 1981. A unique cap(m7GpppXm)-dependent influenza virion endonuclease cleaves capped RNAs to generate the primers that initiate viral RNA transcription. Cell 23:847-58.

45. Guilligay D, Tarendeau F, Resa-Infante P, Coloma R, Crepin T, Sehr P, Lewis J, Ruigrok RW, Ortin J, Hart DJ, Cusack S. 2008. The structural basis for cap binding by influenza virus polymerase subunit PB2. Nat Struct Mol Biol 15:500-6.

46. Yuan P, Bartlam M, Lou Z, Chen S, Zhou J, He X, Lv Z, Ge R, Li X, Deng T, Fodor E, Rao Z, Liu Y. 2009. Crystal structure of an avian influenza polymerase PA(N) reveals an endonuclease active site. Nature 458:909-13.

47. Wu CY, Jeng KS, Lai MM. 2011. The SUMOylation of matrix protein M1 modulates the assembly and morphogenesis of influenza A virus. J Virol 85:6618-28.

48. Rossman JS, Lamb RA. 2011. Influenza virus assembly and budding. Virology 411:229-36.

49. Matsuoka Y, Matsumae H, Katoh M, Eisfeld AJ, Neumann G, Hase T, Ghosh S, Shoemaker JE, Lopes TJ, Watanabe T, Watanabe S, Fukuyama S, Kitano H, Kawaoka Y. 2013. A comprehensive map of the influenza A virus replication cycle. BMC Syst Biol 7:97.

50. Liu C, Eichelberger MC, Compans RW, Air GM. 1995. Influenza type A virus neuraminidase does not play a role in viral entry, replication, assembly, or budding. J Virol 69:1099-106.

51. Robinson KM, Kolls JK, Alcorn JF. 2015. The immunology of influenza virus-associated bacterial pneumonia. Curr Opin Immunol 34:59-67.

52.   McCullers JA. 2014. The co-pathogenesis of influenza viruses with bacteria in the lung. Nat Rev Microbiol 12:252-62.

53.   Rynda-Apple A, Robinson KM, Alcorn JF. 2015. Influenza and Bacterial Superinfection: Illuminating the Immunologic Mechanisms of Disease. Infect Immun 83:3764-70.

54.   Smith AM, McCullers JA. 2014. Secondary bacterial infections in influenza virus infection pathogenesis. Curr Top Microbiol Immunol 385:327-56.

55.   Metzger DW, Sun K. 2013. Immune dysfunction and bacterial coinfections following influenza. J Immunol 191:2047-52.

56.   Henriques-Normark B, Tuomanen EI. 2013. The Pneumococcus: Epidemiology, Microbiology, and Pathogenesis. Cold Spring Harb Perspect Med 3.

57.   Tettelin H, Nelson KE, Paulsen IT, Eisen JA, Read TD, Peterson S, Heidelberg J, DeBoy RT, Haft DH, Dodson RJ, Durkin AS, Gwinn M, Kolonay JF, Nelson WC, Peterson JD, Umayam LA, White O, Salzberg SL, Lewis MR, Radune D, Holtzapple E, Khouri H, Wolf AM, Utterback TR, Hansen CL, McDonald LA, Feldblyum TV, Angiuoli S, Dickinson T, Hickey EK, Holt IE, Loftus BJ, Yang F, Smith HO, Venter JC, Dougherty BA, Morrison DA, Hollingshead SK, Fraser CM. 2001. Complete genome sequence of a virulent isolate of Streptococcus pneumoniae. Science 293:498-506.

58.   Sjostrom K, Spindler C, Ortqvist A, Kalin M, Sandgren A, Kuhlmann-Berenzon S, Henriques-Normark B. 2006. Clonal and capsular types decide whether pneumococci will act as a primary or opportunistic pathogen. Clin Infect Dis 42:451-9.

59.   Berry AM, Paton JC. 2000. Additive Attenuation of Virulence of Streptococcus pneumoniae by Mutation of the Genes Encoding Pneumolysin and Other Putative Pneumococcal Virulence Proteins. Infect Immun 68:133-40.

60.   Nunes S, Sá-Leão R, Carriço J, Alves CR, Mato R, Avô AB, Saldanha J, Almeida JS, Sanches IS, de Lencastre H. 2005. Trends in Drug Resistance, Serotypes, and Molecular Types of Streptococcus pneumoniae Colonizing Preschool-Age Children Attending Day Care Centers in Lisbon, Portugal: a Summary of 4 Years of Annual Surveillance. J Clin Microbiol 43:1285-93.

61.   Högberg L, Geli P, Ringberg H, Melander E, Lipsitch M, Ekdahl K. 2007. Age-
and Serogroup-Related Differences in Observed Durations of Nasopharyngeal
Carriage of Penicillin-Resistant Pneumococci ▿. J Clin Microbiol 45:948-52.

62.   Sandgren A, Albiger B, Orihuela CJ, Tuomanen E, Normark S, Henriques-
Normark B. 2017. Virulence in Mice of Pneumococcal Clonal Types with Known
Invasive Disease Potential in Humans. J Infect Dis 192:791-800.

63.   Bean B, Tomasz A. 1977. Choline metabolism in pneumococci. J Bacteriol
130:571-4.

64.   Cundell DR, Gerard NP, Gerard C, Idanpaan-Heikkila I, Tuomanen EI. 1995.
Streptococcus pneumoniae anchor to activated human cells by the receptor for
platelet-activating factor. Nature 377:435-8.

65.   Canvin JR, Marvin AP, Sivakumaran M, Paton JC, Boulnois GJ, Andrew PW,
Mitchell TJ. 1995. The role of pneumolysin and autolysin in the pathology of
pneumonia and septicemia in mice infected with a type 2 pneumococcus. J Infect
Dis 172:119-23.

66.   Duane PG, Rubins JB, Weisel HR, Janoff EN. 1993. Identification of hydrogen
peroxide as a Streptococcus pneumoniae toxin for rat alveolar epithelial cells.
Infect Immun 61:4392-7.

67.   Rai P, He F, Kwang J, Engelward BP, Chow VT. 2016. Pneumococcal
Pneumolysin Induces DNA Damage and Cell Cycle Arrest. Sci Rep 6:22972.

68.   Pericone CD, Overweg K, Hermans PW, Weiser JN. 2000. Inhibitory and
bactericidal effects of hydrogen peroxide production by Streptococcus
pneumoniae on other inhabitants of the upper respiratory tract. Infect Immun
68:3990-7.

69.   Torres AC, Catia. 2015. Clinical Management of Bacterial Pneumonia. ADIS.

70.   Koppe U, Department of Internal Medicine/Infectious Diseases and Pulmonary
Medicine CUB, Augustenburger Platz 1, 13353 Berlin, Germany., Suttorp N,
Opitz B. 2017. Recognition of Streptococcus pneumoniae by the innate immune
system. Cell Microbiol 14:460-466.

71.   Weiss U. 2008. Inflammation. Nature 454:427.

72.   Taylor BC, Michael. Weitz,Joshua. 2017. The virus of my virus is my friend: Ecological effects of virophage with alternative modes of coinfection - ScienceDirect. J Theor Biol 354.

73.   Smith AM, Adler FR, Ribeiro RM, Gutenkunst RN, McAuley JL, McCullers JA, Perelson AS. 2013. Kinetics of Coinfection with Influenza A Virus and Streptococcus pneumoniae. PLoS Pathog 2013 9:1.

74.   Samokhvalov IM. 2014. Deconvoluting the ontogeny of hematopoietic stem cells. Cell Mol Life Sci 71:957-78.

75.   Nesargikar PN, Spiller B, Chavez R. 2012. The complement system: history, pathways, cascade and inhibitors. Eur J Microbiol Immunol (Bp) 2:103-11.

76.   Okamoto M, Tsukamoto H, Kouwaki T, Seya T, Oshiumi H. 2017. Recognition of Viral RNA by Pattern Recognition Receptors in the Induction of Innate Immunity and Excessive Inflammation During Respiratory Viral Infections. Viral Immunol 30:408-420.

77.   Witzenrath M, Pache F, Lorenz D, Koppe U, Gutbier B, Tabeling C, Reppe K, Meixenberger K, Dorhoi A, Ma J, Holmes A, Trendelenburg G, Heimesaat MM, Bereswill S, van der Linden M, Tschopp J, Mitchell TJ, Suttorp N, Opitz B. 2011. The NLRP3 inflammasome is differentially activated by pneumolysin variants and contributes to host defense in pneumococcal pneumonia. J Immunol 187:434-40.

78.   Brodin P, Davis MM. 2016. Human immune system variation. Nat Rev Immunol 17:21.

79.   Parkin J, Cohen B. 2001. An overview of the immune system. Lancet 357:1777-89.

80.   Sun K, Metzger DW. 2008. Inhibition of pulmonary antibacterial defense by interferon-gamma during recovery from influenza infection. Nat Med 14:558-64.

81.   de Jong MD, Simmons CP, Thanh TT, Hien VM, Smith GJD, Chau TNB, Hoang DM, Van Vinh Chau N, Khanh TH, Dong VC, Qui PT, Van Cam B, Ha DQ,

Guan Y, Peiris JSM, Chinh NT, Hien TT, Farrar J. 2006. Fatal outcome of human influenza A (H5N1) is associated with high viral load and hypercytokinemia. Nat Med 12:1203-7.

82. Hashimoto Y, Moki T, Takizawa T, Shiratsuchi A, Nakanishi Y. 2007. Evidence for phagocytosis of influenza virus-infected, apoptotic cells by neutrophils and macrophages in mice. J Immunol 178:2448-57.

83. Kim HM, Lee YW, Lee KJ, Kim HS, Cho SW, van Rooijen N, Guan Y, Seo SH. 2008. Alveolar macrophages are indispensable for controlling influenza viruses in lungs of pigs. J Virol 82:4265-74.

84. Herold S, von Wulffen W, Steinmueller M, Pleschka S, Kuziel WA, Mack M, Srivastava M, Seeger W, Maus UA, Lohmeyer J. 2006. Alveolar epithelial cells direct monocyte transepithelial migration upon influenza virus infection: impact of chemokines and adhesion molecules. J Immunol 177:1817-24.

85. Mendelson M, Tekoah Y, Zilka A, Gershoni-Yahalom O, Gazit R, Achdout H, Bovin NV, Meningher T, Mandelboim M, Mandelboim O, David A, Porgador A. 2010. NKp46 O-glycan sequences that are involved in the interaction with hemagglutinin type 1 of influenza virus. J Virol 84:3789-97.

86. Bhardwaj N, Bender A, Gonzalez N, Bui LK, Garrett MC, Steinman RM. 1994. Influenza virus-infected dendritic cells stimulate strong proliferative and cytolytic responses from human CD8+ T cells. J Clin Invest 94:797-807.

87. Heer AK, Harris NL, Kopf M, Marsland BJ. 2008. CD4+ and CD8+ T cells exhibit differential requirements for CCR7-mediated antigen transport during influenza infection. J Immunol 181:6984-94.

88. Yu X, Tsibane T, McGraw PA, House FS, Keefer CJ, Hicar MD, Tumpey TM, Pappas C, Perrone LA, Martinez O, Stevens J, Wilson IA, Aguilar PV, Altschuler EL, Basler CF, Crowe JE, Jr. 2008. Neutralizing antibodies derived from the B cells of 1918 influenza pandemic survivors. Nature 455:532-6.

89. Schulman JL, Khakpour M, Kilbourne ED. 1968. Protective effects of specific immunity to viral neuraminidase on influenza virus infection of mice. J Virol 2:778-86.

90.   Treanor JJ, Tierney EL, Zebedee SL, Lamb RA, Murphy BR. 1990. Passively transferred monoclonal antibody to the M2 protein inhibits influenza A virus replication in mice. J Virol 64:1375-7.

91.   Sukeno N, Otsuki Y, Konno J, Yamane N, Odagiri T, Arikawa J, Ishida N. 1979. Anti-nucleoprotein antibody response in influenza A infection. Tohoku J Exp Med 128:241-9.

92.   Nakanishi Y, Lu B, Gerard C, Iwasaki A. 2009. CD8(+) T lymphocyte mobilization to virus-infected tissue requires CD4(+) T-cell help. Nature 462:510-3.

93.   Brown DM, Roman E, Swain SL. 2004. CD4 T cell responses to influenza infection. Semin Immunol 16:171-7.

94.   Surls J, Nazarov-Stoica C, Kehl M, Casares S, Brumeanu TD. 2010. Differential effect of CD4+Foxp3+ T-regulatory cells on the B and T helper cell responses to influenza virus vaccination. Vaccine 28:7319-30.

95.   Bermejo-Martin JF, Ortiz de Lejarazu R, Pumarola T, Rello J, Almansa R, Ramirez P, Martin-Loeches I, Varillas D, Gallegos MC, Seron C, Micheloud D, Gomez JM, Tenorio-Abreu A, Ramos MJ, Molina ML, Huidobro S, Sanchez E, Gordon M, Fernandez V, Del Castillo A, Marcos MA, Villanueva B, Lopez CJ, Rodriguez-Dominguez M, Galan JC, Canton R, Lietor A, Rojo S, Eiros JM, Hinojosa C, Gonzalez I, Torner N, Banner D, Leon A, Cuesta P, Rowe T, Kelvin DJ. 2009. Th1 and Th17 hypercytokinemia as early host response signature in severe pandemic influenza. Crit Care 13:R201.

96.   Loo YM, Gale M. 2011. Immune signaling by RIG-I-like receptors. Immunity 34:680-92.

97.   Cui Sea. 2008. The C-terminal regulatory domain is the RNA 5'triphosphate sensor of RIG-I. Molecular Cell 29:169 - 179

98.   Pothlichet J, Burtey A, Kubarenko AV, Caignard G, Solhonne B, Tangy F, Ben-Ali M, Quintana-Murci L, Heinzmann A, Chiche JD, Vidalain PO, Weber AN, Chignard M, Si-Tahar M. 2009. Study of human RIG-I polymorphisms identifies two variants with an opposite impact on the antiviral immune response. PLoS One 4:e7582.

99. Fredericksen BL, Gale M, Jr. 2006. West Nile virus evades activation of interferon regulatory factor 3 through RIG-I-dependent and -independent pathways without antagonizing host defense signaling. J Virol 80:2913-23.

100. Zhong Y, Kinio A, Saleh M. 2013. Functions of NOD-Like Receptors in Human Diseases. Front Immunol 4.

101. Liu X, Chauhan VS, Young AB, Marriott I. 2010. NOD2 mediates inflammatory responses of primary murine glia to Streptococcus pneumoniae. Glia 58:839-47.

102. Opitz B, Puschel A, Schmeck B, Hocke AC, Rosseau S, Hammerschmidt S, Schumann RR, Suttorp N, Hippenstiel S. 2004. Nucleotide-binding oligomerization domain proteins are innate immune receptors for internalized Streptococcus pneumoniae. J Biol Chem 279:36426-32.

103. Hommes TJ, van Lieshout MH, van 't Veer C, Florquin S, Bootsma HJ, Hermans PW, de Vos AF, van der Poll T. 2015. Role of Nucleotide-Binding Oligomerization Domain-Containing (NOD) 2 in Host Defense during Pneumococcal Pneumonia. PLoS One 10.

104. Sorbara MT, Philpott DJ. 2011. Peptidoglycan: a critical activator of the mammalian immune system during infection and homeostasis. Immunol Rev 243:40-60.

105. Yoshimura A, Lien E, Ingalls RR, Tuomanen E, Dziarski R, Golenbock D. 1999. Cutting edge: recognition of Gram-positive bacterial cell wall components by the innate immune system occurs via Toll-like receptor 2. J Immunol 163:1-5.

106. Dessing MC, Sluijs KFvd, Florquin S, Akira S, Poll Tvd. 2007. Toll-Like Receptor 2 Does Not Contribute to Host Response during Postinfluenza Pneumococcal Pneumonia. Am J Respir Cell Mol 36:609-614.

107. Koymans KJ, Goldmann O, Karlsson CAQ, Sital W, Thanert R, Bisschop A, Vrieling M, Malmstrom J, van Kessel KPM, de Haas CJC, van Strijp JAG, Medina E. 2017. The TLR2 Antagonist Staphylococcal Superantigen-Like Protein 3 Acts as a Virulence Factor to Promote Bacterial Pathogenicity in vivo. J Innate Immun doi:10.1159/000479100.

108. van Rossum AM, Lysenko ES, Weiser JN. 2005. Host and bacterial factors contributing to the clearance of colonization by Streptococcus pneumoniae in a murine model. Infect Immun 73:7718-26.

109. Mogensen TH, Paludan SR, Kilian M, Ostergaard L. 2006. Live Streptococcus pneumoniae, Haemophilus influenzae, and Neisseria meningitidis activate the inflammatory response through Toll-like receptors 2, 4, and 9 in species-specific patterns. J Leukoc Biol 80:267-77.

110. Guillot L, Le Goffic R, Bloch S, Escriou N, Akira S, Chignard M, Si-Tahar M. 2005. Involvement of toll-like receptor 3 in the immune response of lung epithelial cells to double-stranded RNA and influenza A virus. J Biol Chem 280:5571-80.

111. Spelmink L, Sender V, Hentrich K, Kuri T, Plant L, Henriques-Normark B. 2016. Toll-Like Receptor 3/TRIF-Dependent IL-12p70 Secretion Mediated by Streptococcus pneumoniae RNA and Its Priming by Influenza A Virus Coinfection in Human Dendritic Cells. mBio 7:168-16

112. Perales-Linares R, Navas-Martin S. 2013. Toll-like receptor 3 in viral pathogenesis: friend or foe? Immunology 140:153-67.

113. Le Goffic R, Balloy V, Lagranderie M, Alexopoulou L, Escriou N, Flavell R, Chignard M, Si-Tahar M. 2006. Detrimental contribution of the Toll-like receptor (TLR)3 to influenza A virus-induced acute pneumonia. PLoS Pathog 2:e53.

114. Diebold SS, Kaisho T, Hemmi H, Akira S, Reis e Sousa C. 2004. Innate antiviral responses by means of TLR7-mediated recognition of single-stranded RNA. Science 303:1529-31.

115. Miettinen M, Sareneva T, Julkunen I, Matikainen S. 2001. IFNs activate toll-like receptor gene expression in viral infections. Genes Immun 2:349-55.

116. Stegemann-Koniszewski S, Gereke M, Orrskog S, Lienenklaus S, Pasche B, Bader SR, Gruber AD, Akira S, Weiss S, Henriques-Normark B, Bruder D, Gunzer M. 2013. TLR7 contributes to the rapid progression but not to the overall fatal outcome of secondary pneumococcal disease following influenza A virus infection. J Innate Immun 5:84-96.

117. Sun Q, Sun L, Liu HH, Chen X, Seth RB, Forman J, Chen ZJ. 2006. The specific and essential role of MAVS in antiviral innate immune responses. Immunity 24:633-42.

118. Lupfer C, Thomas PG, Anand PK, Vogel P, Milasta S, Martinez J, Huang G, Green M, Kundu M, Chi H, Xavier RJ, Green DR, Lamkanfi M, Dinarello CA, Doherty PC, Kanneganti TD. 2013. Receptor interacting protein kinase 2-mediated mitophagy regulates inflammasome activation during virus infection. Nat Immunol 14:480-8.

119. van Lieshout MHP, de Vos AF, Dessing MC, de Porto A, de Boer OJ, de Beer R, Terpstra S, Florquin S, Van't Veer C, van der Poll T. 2017. ASC and NLRP3 impair host defense during lethal pneumonia caused by serotype 3 Streptococcus pneumoniae in mice. Eur J Immunol doi:10.1002/eji.201646554.

120. von Bernuth H, Picard C, Jin Z, Pankla R, Xiao H, Ku CL, Chrabieh M, Mustapha IB, Ghandil P, Camcioglu Y, Vasconcelos J, Sirvent N, Guedes M, Vitor AB, Herrero-Mata MJ, Arostegui JI, Rodrigo C, Alsina L, Ruiz-Ortiz E, Juan M, Fortuny C, Yague J, Anton J, Pascal M, Chang HH, Janniere L, Rose Y, Garty BZ, Chapel H, Issekutz A, Marodi L, Rodriguez-Gallego C, Banchereau J, Abel L, Li X, Chaussabel D, Puel A, Casanova JL. 2008. Pyogenic bacterial infections in humans with MyD88 deficiency. Science 321:691-6.

121. Koedel U, Rupprecht T, Angele B, Heesemann J, Wagner H, Pfister HW, Kirschning CJ. 2004. MyD88 is required for mounting a robust host immune response to Streptococcus pneumoniae in the CNS. Brain 127:1437-45.

122. Deguine J, Barton GM. 2014. MyD88: a central player in innate immune signaling. F1000Prime Rep 6:97.

123. Akira MY, Shintaro S, Kiyotoshi M, Katsuaki H, Osamu T, Kiyoshi T, Shizuo. 2002. Cutting Edge: A Novel Toll/IL-1 Receptor Domain-Containing Adapter That Preferentially Activates the IFN-β Promoter in the Toll-Like Receptor Signaling. J Immunol 169: 6668-6672.

124. Esposito S, Molteni CG, Giliani S, Mazza C, Scala A, Tagliaferri L, Pelucchi C, Fossali E, Plebani A, Principi N. 2012. Toll-like receptor 3 gene polymorphisms and severity of pandemic A/H1N1/2009 influenza in otherwise healthy children. Virol J 9:270.

125. Muzio M, Ni J, Feng P, Dixit VM. 2013. Pillars article: IRAK (Pelle) family member IRAK-2 and MyD88 as proximal mediators of IL-1 signaling. Science. 1997. 278: 1612-1615. J Immunol 190:16-9.

126. Yaron A, Hatzubai A, Davis M, Lavon I, Amit S, Manning AM, Andersen JS, Mann M, Mercurio F, Ben-Neriah Y. 1998. Identification of the receptor component of the IkappaBalpha-ubiquitin ligase. Nature 396:590-4.

127. Huang DB, Huxford T, Chen YQ, Ghosh G. 1997. The role of DNA in the mechanism of NFkappaB dimer formation: crystal structures of the dimerization domains of the p50 and p65 subunits. Structure 5:1427-36.

128. McComb S, Cessford E, Alturki NA, Joseph J, Shutinoski B, Startek JB, Gamero AM, Mossman KL, Sad S. 2014. Type-I interferon signaling through ISGF3 complex is required for sustained Rip3 activation and necroptosis in macrophages. Proc. Natl. Acad. Sci. U.S.A. 111:E3206-E3213.

129. Au-Yeung N, Mandhana R, Horvath CM. 2013. Transcriptional regulation by STAT1 and STAT2 in the interferon JAK-STAT pathway. JAKSTAT 2:e23931.

130. Meraz MA, White JM, Sheehan KC, Bach EA, Rodig SJ, Dighe AS, Kaplan DH, Riley JK, Greenlund AC, Campbell D, Carver-Moore K, DuBois RN, Clark R, Aguet M, Schreiber RD. 1996. Targeted disruption of the Stat1 gene in mice reveals unexpected physiologic specificity in the JAK-STAT signaling pathway. Cell 84:431-42.

131. Shahangian A, Chow EK, Tian X, Kang JR, Ghaffari A, Liu SY, Belperio JA, Cheng G, Deng JC. 2009. Type I IFNs mediate development of postinfluenza bacterial pneumonia in mice. J Clin Invest 119:1910-20 .

132. Nakamura S, Davis KM, Weiser JN. 2011. Synergistic stimulation of type I interferons during influenza virus coinfection promotes Streptococcus pneumoniae colonization in mice. J Clin Invest 121:3657.

133. Kudva A, Scheller EV, Robinson KM, Crowe CR, Choi SM, Slight SR, Khader SA, Dubin PJ, Enelow RI, Kolls JK, Alcorn JF. 2011. Influenza A inhibits Th17-mediated host defense against bacterial pneumonia in mice. J Immunol 186:1666-1674.

134. Lee B, Robinson KM, McHugh KJ, Scheller EV, Mandalapu S, Chen C, Di YP, Clay ME, Enelow RI, Dubin PJ, Alcorn JF. 2015. Influenza-induced type I interferon enhances susceptibility to gram-negative and gram-positive bacterial pneumonia in mice. Am J Physiol Lung Cell Mol Physiol 309:L158-67.

135. Smith AM, Smith AP. 2016. A Critical, Nonlinear Threshold Dictates Bacterial Invasion and Initial Kinetics During Influenza. Sci Rep 6:38703.

136. Jakab GJ. 1982. Immune impairment of alveolar macrophage phagocytosis during influenza virus pneumonia. Am Rev Respir Dis 126:778-82.

137. Mina MJ, Brown LA, Klugman KP. 2015. Dynamics of Increasing IFN-gamma Exposure on Murine MH-S Cell-Line Alveolar Macrophage Phagocytosis of Streptococcus pneumoniae. J Interferon Cytokine Res 35:474-9.

138. Sharma-Chawla N, Sender V, Kershaw O, Gruber AD, Volckmar J, Henriques-Normark B, Stegemann-Koniszewski S, Bruder D. 2016. Influenza A Virus Infection Predisposes Hosts to Secondary Infection with Different Streptococcus pneumoniae Serotypes with Similar Outcome but Serotype-Specific Manifestation. Infect Immun 84:3445-3457.

139. Scheller J, Chalaris A, Schmidt-Arras D, Rose-John S. 2011. The pro- and anti-inflammatory properties of the cytokine interleukin-6. Biochim Biophys Acta 1813:878-888.

140. Wilson KP, Black J-AF, Thomson JA, Kim EE, Griffith JP, Navia MA, Murcko MA, Chambers SP, Aldape RA, Raybuck SA, Livingston DJ. 1994. Structure and mechanism of interleukin-lβ converting enzyme. Nature 370:270.

141. Dinarello CA. 2009. Immunological and inflammatory functions of the interleukin-1 family. Annu Rev Immunol 27:519-50.

142. Voronov E, Carmi Y, Apte RN. 2014. The role IL-1 in tumor-mediated angiogenesis. Front Physiol 5.

143. Thomas PG, Dash P, Aldridge JR, Jr., Ellebedy AH, Reynolds C, Funk AJ, Martin WJ, Lamkanfi M, Webby RJ, Boyd KL, Doherty PC, Kanneganti TD. 2009. The intracellular sensor NLRP3 mediates key innate and healing responses to influenza A virus via the regulation of caspase-1. Immunity 30:566-75.

144. Ghosh SHM. 2011. Celebrating 25 years of NF-[kappa]B. Nat. Immunol 12:681-681.

145. Kanneganti TD, Body-Malapel M, Amer A, Park JH, Whitfield J, Franchi L, Taraporewala ZF, Miller D, Patton JT, Inohara N, Nunez G. 2006. Critical role for Cryopyrin/Nalp3 in activation of caspase-1 in response to viral infection and double-stranded RNA. J Biol Chem 281:36560-8.

146. Ichinohe T, Lee HK, Ogura Y, Flavell R, Iwasaki A. 2009. Inflammasome recognition of influenza virus is essential for adaptive immune responses. J Exp Med 206:79-87.

147. Allen IC, Scull MA, Moore CB, Holl EK, McElvania-TeKippe E, Taxman DJ, Guthrie EH, Pickles RJ, Ting JP. 2009. The NLRP3 inflammasome mediates in vivo innate immunity to influenza A virus through recognition of viral RNA. Immunity 30:556-65.

148. Fang R, Tsuchiya K, Kawamura I, Shen Y, Hara H, Sakai S, Yamamoto T, Fernandes-Alnemri T, Yang R, Hernandez-Cuellar E, Dewamitta SR, Xu Y, Qu H, Alnemri ES, Mitsuyama M. 2011. Critical roles of ASC inflammasomes in caspase-1 activation and host innate resistance to Streptococcus pneumoniae infection. J Immunol 187:4890-9.

149. Ichinohe T, Pang IK, Iwasaki A. 2010. Influenza virus activates inflammasomes via its intracellular M2 ion channel. Nat Immunol 11:404-10.

150. Fang R, Hara H, Sakai S, Hernandez-Cuellar E, Mitsuyama M, Kawamura I, Tsuchiya K. 2014. Type I interferon signaling regulates activation of the absent in melanoma 2 inflammasome during Streptococcus pneumoniae infection. Infect Immun 82:2310-7.

151. Shi J, Zhao Y, Wang K, Shi X, Wang Y, Huang H, Zhuang Y, Cai T, Wang F, Shao F. 2015. Cleavage of GSDMD by inflammatory caspases determines pyroptotic cell death. Nature 526:660-5.

152. Kayagaki N, Stowe IB, Lee BL, O'Rourke K, Anderson K, Warming S, Cuellar T, Haley B, Roose-Girma M, Phung QT, Liu PS, Lill JR, Li H, Wu J, Kummerfeld S, Zhang J, Lee WP, Snipas SJ, Salvesen GS, Morris LX, Fitzgerald L, Zhang Y, Bertram EM, Goodnow CC, Dixit VM. 2015. Caspase-11 cleaves gasdermin D for non-canonical inflammasome signalling. Nature 526:666-71.

153. He WT, Wan H, Hu L, Chen P, Wang X, Huang Z, Yang ZH, Zhong CQ, Han J. 2015. Gasdermin D is an executor of pyroptosis and required for interleukin-1β secretion. Cell Res 25:1285-98.

154. Latz E, Xiao TS, Stutz A. 2013. Activation and regulation of the inflammasomes. Nat Rev Immunol 13.

155. van de Sandt CE, Kreijtz JH, Rimmelzwaan GF. 2012. Evasion of influenza A viruses from innate and adaptive immune responses. Viruses 4:1438-76.

156. Solorzano A, Webby RJ, Lager KM, Janke BH, Garcia-Sastre A, Richt JA. 2005. Mutations in the NS1 protein of swine influenza virus impair anti-interferon activity and confer attenuation in pigs. J Virol 79:7535-43.

157. Boliar S, Chambers TM. 2010. A new strategy of immune evasion by influenza A virus: inhibition of monocyte differentiation into dendritic cells. Vet Immunol Immunopathol 136:201-10.

158. Graef KM, Vreede FT, Lau YF, McCall AW, Carr SM, Subbarao K, Fodor E. 2010. The PB2 subunit of the influenza virus RNA polymerase affects virulence by interacting with the mitochondrial antiviral signaling protein and inhibiting expression of beta interferon. J Virol 84:8433-45.

159. Varga ZT, Ramos I, Hai R, Schmolke M, Garcia-Sastre A, Fernandez-Sesma A, Palese P. 2011. The influenza virus protein PB1-F2 inhibits the induction of type I interferon at the level of the MAVS adaptor protein. PLoS Pathog 7:e1002067.

160. Dias A, Bouvier D, Crepin T, McCarthy AA, Hart DJ, Baudin F, Cusack S, Ruigrok RW. 2009. The cap-snatching endonuclease of influenza virus polymerase resides in the PA subunit. Nature 458:914-8.

161. Mao H, Tu W, Qin G, Law HK, Sia SF, Chan PL, Liu Y, Lam KT, Zheng J, Peiris M, Lau YL. 2009. Influenza virus directly infects human natural killer cells and induces cell apoptosis. J Virol 83:9215-22.

162. van de Sandt CE, Kreijtz J, Rimmelzwaan GF. 2012. Evasion of Influenza A Viruses from Innate and Adaptive Immune Responses. Viruses 4:1438-76.

163.   Smith DJ, Lapedes AS, de Jong JC, Bestebroer TM, Rimmelzwaan GF, Osterhaus AD, Fouchier RA. 2004. Mapping the antigenic and genetic evolution of influenza virus. Science 305:371-6.

164.   De Jong JC, Rimmelzwaan GF, Fouchier RA, Osterhaus AD. 2000. Influenza virus: a master of metamorphosis. J Infect 40:218-28.

165.   Berkhoff EG, de Wit E, Geelhoed-Mieras MM, Boon AC, Symons J, Fouchier RA, Osterhaus AD, Rimmelzwaan GF. 2005. Functional constraints of influenza A virus epitopes limit escape from cytotoxic T lymphocytes. J Virol 79:11239-46.

166.   Andre GO, Converso TR, Politano WR, Ferraz LF, Ribeiro ML, Leite LC, Darrieux M. 2017. Role of Streptococcus pneumoniae Proteins in Evasion of Complement-Mediated Immunity. Front Microbiol 8:224.

167.   Hyams C, Camberlein E, Cohen JM, Bax K, Brown JS. 2010. The Streptococcus pneumoniae capsule inhibits complement activity and neutrophil phagocytosis by multiple mechanisms. Infect Immun 78:704-15.

168.   Mukerji R, Mirza S, Roche AM, Widener RW, Croney CM, Rhee DK, Weiser JN, Szalai AJ, Briles DE. 2012. Pneumococcal surface protein A inhibits complement deposition on the pneumococcal surface by competing with the binding of C-reactive protein to cell-surface phosphocholine. J Immunol 189:5327-35.

169.   Yuste J, Botto M, Paton JC, Holden DW, Brown JS. 2005. Additive inhibition of complement deposition by pneumolysin and PspA facilitates Streptococcus pneumoniae septicemia. J Immunol 175:1813-9.

170.   Dalia AB, Standish AJ, Weiser JN. 2010. Three surface exoglycosidases from Streptococcus pneumoniae, NanA, BgaA, and StrH, promote resistance to opsonophagocytic killing by human neutrophils. Infect Immun 78:2108-16.

171.   McCullers JA, Rehg JE. 2002. Lethal synergism between influenza virus and Streptococcus pneumoniae: characterization of a mouse model and the role of platelet-activating factor receptor. J Infect Dis 186:341-50.

172.   Nita-Lazar M, Banerjee A, Feng C, Amin MN, Frieman MB, Chen WH, Cross AS, Wang LX, Vasta GR. 2015. Desialylation of airway epithelial cells during influenza virus infection enhances pneumococcal adhesion via galectin binding. Mol Immunol 65:1-16.

173.	Pittet LA, Hall-Stoodley L, Rutkowski MR, Harmsen AG. 2010. Influenza virus infection decreases tracheal mucociliary velocity and clearance of Streptococcus pneumoniae. Am J Respir Cell Mol Biol 42:450-60.

174.	Ghoneim HE, Thomas PG, McCullers JA. 2013. Depletion of alveolar macrophages during influenza infection facilitates bacterial superinfections. J Immunol 191:1250-9.

175.	Hartshorn KL, Liou LS, White MR, Kazhdan MM, Tauber JL, Tauber AI. 1995. Neutrophil deactivation by influenza A virus. Role of hemagglutinin binding to specific sialic acid-bearing cellular proteins. J Immunol 154:3952-60.

176.	Peltola VT, McCullers JA. 2004. Respiratory viruses predisposing to bacterial infections: role of neuraminidase. Pediatr Infect Dis J 23:S87-97.

177.	Colamussi ML, White MR, Crouch E, Hartshorn KL. 1999. Influenza A virus accelerates neutrophil apoptosis and markedly potentiates apoptotic effects of bacteria. Blood 93:2395-403.

178.	Lynnelle A. McNamee AGH. 2006. Both Influenza-Induced Neutrophil Dysfunction and Neutrophil-Independent Mechanisms Contribute to Increased Susceptibility to a Secondary Streptococcus pneumoniae Infection Infection and Immunity 74:6707–6721.

179.	Engelich G WM, Hartshorn KL. 2001. Neutrophil survival is markedly reduced by incubation with influenza virus and Streptococcus pneumoniae: role of respiratory burst. J Leukoc Biol 69:50-6.

180.	LeVine AM, Koeningsknecht V, Stark JM. 2001. Decreased pulmonary clearance of S. pneumoniae following influenza A infection in mice. J Virol Methods 94:173-86.

181.	McCullers JA. 2004. Effect of Antiviral Treatment on the Outcome of Secondary Bacterial Pneumonia after Influenza. J Infect Dis 190:519-526.

182.	Karlstrom A, Boyd KL, English BK, McCullers JA. 2009. Treatment with protein synthesis inhibitors improves outcomes of secondary bacterial pneumonia after influenza. J Infect Dis 199:311-9.

183.   Nedel WL, Nora DG, Salluh JIF, Lisboa T, Póvoa P. 2016. Corticosteroids for severe influenza pneumonia: A critical appraisal. World J Crit Care Med 5:89-95.

184.   Karunanithi K, V A, J AK, Mohan N, Kumar A, Kuriakose E, Kumar D, Kavitha S, P ST, Kumar G. 2017. Role of Corticosteroids in Influenza Pneumonia (H1N1) Patients. Universal Journal of Medical Science doi:10.13189/ujmsj.2015.030401.

185.   Han K, Ma H, An X, Su Y, Chen J, Lian Z, Zhao J, Zhu BP, Fontaine RE, Feng Z, Zeng G. 2011. Early use of glucocorticoids was a risk factor for critical disease and death from pH1N1 infection. Clin Infect Dis 53:326-33.

186.   Rudd JM, Ashar HK, Chow VT, Teluguakula N. 2016. Lethal Synergism between Influenza and Streptococcus pneumoniae. J Infect Pulm Dis 2.

187.   Lupfer CR, Anand PK, Liu Z, Stokes KL, Vogel P, Lamkanfi M, Kanneganti TD. 2014. Reactive Oxygen Species Regulate Caspase-11 Expression and Activation of the Non-canonical NLRP3 Inflammasome during Enteric Pathogen Infection. PLoS Pathog 10.

188.   Shahangian A, Chow EK, Tian X, Kang JR, Ghaffari A, Liu SY, Belperio JA, Cheng G, Deng JC. 2009. Type I IFNs mediate development of postinfluenza bacterial pneumonia in mice. J Clin Invest 119:1910-20.

189.   Lupfer C, Stein DA, Mourich DV, Tepper SE, Iversen PL, Pastey M. 2008. Inhibition of influenza A H3N8 virus infections in mice by morpholino oligomers. Arch Virol 153:929-37.

190.   van der Sluijs KF, van Elden LJ, Nijhuis M, Schuurman R, Pater JM, Florquin S, Goldman M, Jansen HM, Lutter R, van der Poll T. 2004. IL-10 is an important mediator of the enhanced susceptibility to pneumococcal pneumonia after influenza infection. J Immunol 172:7603-9.

191.   Bauernfeind FG, Horvath G, Stutz A, Alnemri ES, MacDonald K, Speert D, Fernandes-Alnemri T, Wu J, Monks BG, Fitzgerald KA, Hornung V, Latz E. 2009. Cutting edge: NF-kappaB activating pattern recognition and cytokine receptors license NLRP3 inflammasome activation by regulating NLRP3 expression. J Immunol 183:787-91.

192.   Ghosh CC, Ramaswami S, Juvekar A, Vu HY, Galdieri L, Davidson D, Vancurova I. 2010. Gene-specific repression of proinflammatory cytokines in

stimulated human macrophages by nuclear IkappaBalpha. J Immunol 185:3685-93.

193. Zhang H, Luo J, Alcorn JF, Chen K, Fan S, Pilewski J, Liu A, Chen W, Kolls JK, Wang J. 2017. AIM2 Inflammasome Is Critical for Influenza-Induced Lung Injury and Mortality. J Immunol 198:4383-93.

194. Casalino E, Antoniol S, Fidouh N, Choquet C, Lucet JC, Duval X, Visseaux B, Pereira L. 2017. Influenza virus infections among patients attending emergency department according to main reason to presenting to ED: A 3-year prospective observational study during seasonal epidemic periods. PLoS One 12:e0182191.

195. Smith MW, Schmidt JE, Rehg JE, Orihuela CJ, McCullers JA. 2007. Induction of Pro- and Anti-inflammatory Molecules in a Mouse Model of Pneumococcal Pneumonia after Influenza. Comp Med 57:82-9.

196. Garlanda C, Dinarello CA, Mantovani A. 2013. The interleukin-1 family: back to the future. Immunity 39:1003-18.

197. Krelin Y, Voronov E, Dotan S, Elkabets M, Reich E, Fogel M, Huszar M, Iwakura Y, Segal S, Dinarello CA, Apte RN. 2007. Interleukin-1β–Driven Inflammation Promotes the Development and Invasiveness of Chemical Carcinogen–Induced Tumors. Cancer Res 67:1062-1071.

198. Goldbach-Mansky R, Dailey NJ, Canna SW, Gelabert A, Jones J, Rubin BI, Kim HJ, Brewer C, Zalewski C, Wiggs E, Hill S, Turner ML, Karp BI, Aksentijevich I, Pucino F, Penzak SR, Haverkamp MH, Stein L, Adams BS, Moore TL, Fuhlbrigge RC, Shaham B, Jarvis JN, O'Neil K, Vehe RK, Beitz LO, Gardner G, Hannan WP, Warren RW, Horn W, Cole JL, Paul SM, Hawkins PN, Pham TH, Snyder C, Wesley RA, Hoffmann SC, Holland SM, Butman JA, Kastner DL. 2006. Neonatal-onset multisystem inflammatory disease responsive to interleukin-1beta inhibition. N Engl J Med 355:581-92.

199. Dinarello CA. 1996. Biologic basis for interleukin-1 in disease. Blood 87:2095-147.

200. Warner N, Nunez G. 2013. MyD88: a critical adaptor protein in innate immunity signal transduction. J Immunol 190:3-4.

201.   Chang J, Kunkel SL, Chang CH. 2009. Negative regulation of MyD88-dependent signaling by IL-10 in dendritic cells. Proc Natl Acad Sci U S A 106:18327-32.

202.   Barthelemy A, Ivanov S, Fontaine J, Soulard D, Bouabe H, Paget C, Faveeuw C, Trottein F. 2017. Influenza A virus-induced release of interleukin-10 inhibits the anti-microbial activities of invariant natural killer T cells during invasive pneumococcal superinfection. Mucosal Immunol 10:460-469.

203.   McCullers JA, Bartmess KC. 2003. Role of neuraminidase in lethal synergism between influenza virus and Streptococcus pneumoniae. J Infect Dis 187:1000-9.

Table 1. Western blot antibodies. Membrane was incubated with primary antibody overnight. Secondary antibody was added the following day. Antibodies were selected depending on the protein of interest.

Western Blot Antibodies		
Primary antibody	Secondary Antibody	Purchased from
anti-β-Actin (D6A8)	anti-rabbit HRP secondary antibody	Cell signaling technologies
IL-1β (D3H1Z)	anti-rabbit HRP secondary antibody	Cell signaling technologies
phosphorylated-IκBα,Ser32 (14D4)	anti-rabbit HRP secondary antibody	Cell signaling technologies
IκBα antibody (9242)	anti-rabbit HRP secondary antibody	Cell signaling technologies
Anti-caspase-1(p20 mouse)	anti-mouse HRP secondary antibody	Adipogene, AG-20B-0042-C100

Table 2. Fluorescent antibodies. The fluorophores detect specific cell receptors. These receptors represent a cell population.

Fluorescent antibodies

Chanel	Fluorophore	Monocyte Receptor	Represents	Lymphocyte Receptor	Represents
FL-1	FITC	CD11c	Dendritic cells	CD4	CD4 T cells
FL-2	PE	GR1	Neutrophils	CD8	CD8 T cells
FL-3	PerCP	TCR-β	T cells	TCR-β	T cells
FL-4	APC	CD11b	Macrophages	CD19	B cells

Table 3. Histological Scoring. Lungs collected from infected mice were analyzed by a pathologist and scored based on different characteristics.

	Histological Score			
Score	infiltrate of neutrophils	infiltrate of lymphocytes	airways	Architecture
0	No significant abnormality.	No significant abnormality.	unremarkable airways	intact alveolar architecture
1	Very patchy moderate	Very patchy moderate	early plugging	mostly intact
2	Mild patchy infiltrate	Mild patchy infiltrate	plugging	inflamed airways
3	Mild fairly diffuse	Mild fairly diffuse	early obliteration	architectural breakdown
4	Patchy moderate	Patchy moderate	diffuse obliteration of airways	severe architectural breakdown
5	Moderate mixed	Moderate mixed		tissue mostly lost.
6	Marked infiltrate	Marked infiltrate		
	YES (+1) / NO (0)			
Alveolar hemorrhage				
Necrosis				
				Overall Score ____/27

Table 4. Real Time-qPCR primer sequences. Forward and reverse primers were added to a master mix depending on the mRNA of interest.

	Real Time-qPCR primer sequences	
Primer	Forward	Reverse
β-Actin	FW 5'- GGC TGT ATT CCC CTC CAT CG-3'	Rev 5'-CCA GTT GTT AAC AAT GCC ATG T-3'
IL-1β	FW 5' GAC CTT CCA GGA TGA GGA CA -3'	Rev 5' AGC TCA TAT GGG TCC GAC AG-3'
TNF-α	FW 5'-CAT CTT CTC AAA ATT CGA GTG ACA A- 3'	Rev 5'-TGG GAG TAG ACA AGG TAC AAC CC-3'
IL-6	FW 5'- TCC AGT TGC CTT CTT GGG AC -3'	Rev 5'- GTA CTC CAG AAG ACC AGA GG -3'
MYD88	FW 5' –ATC CGA GAG CTG GAA ACG-3'	Rev 5' GCA AGG GTT GGT ATA ATC-3'
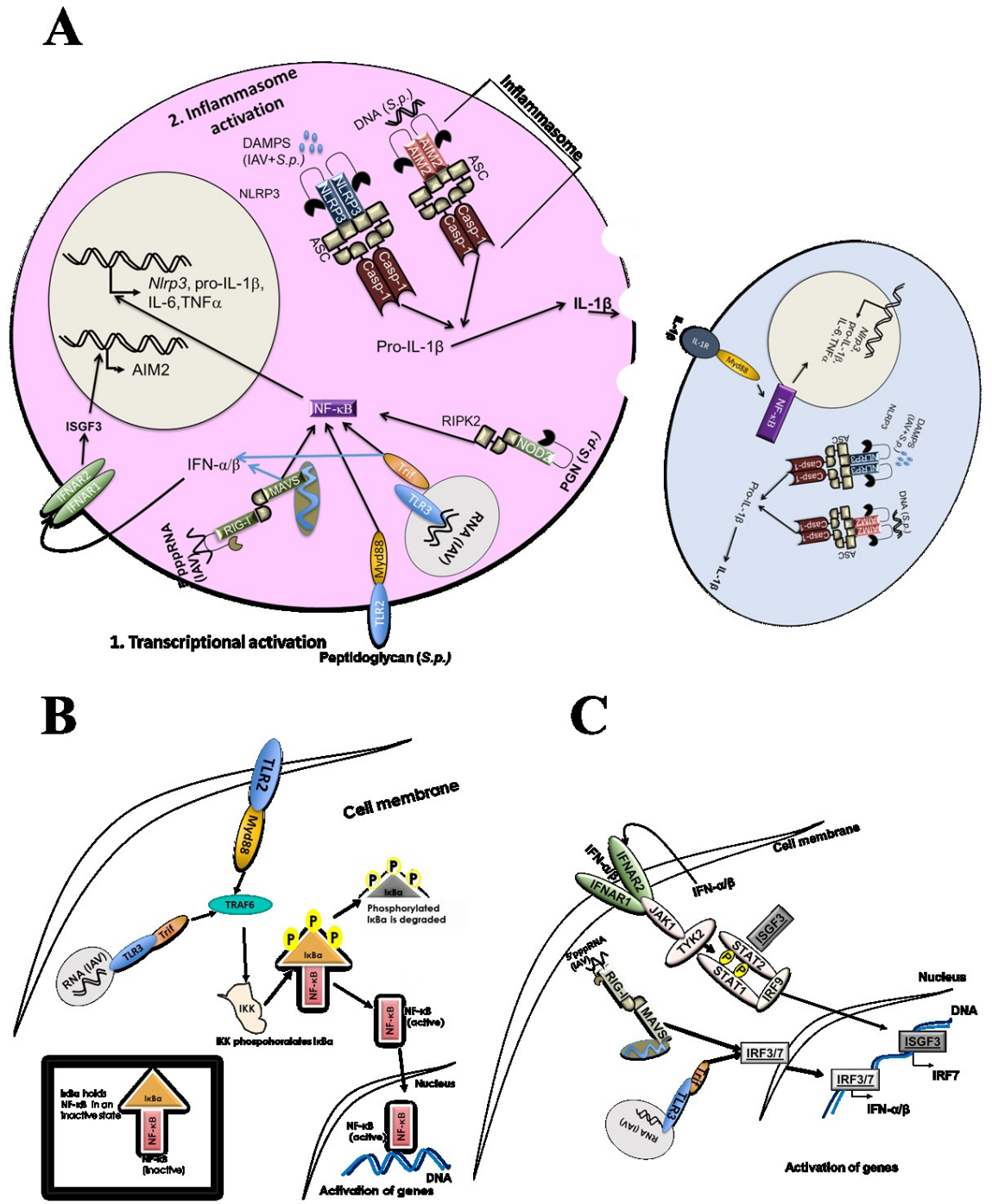
Figure 1. Proposed signaling pathway. A) Proposed signaling pathway of the coinfection with IAV and *S. pneumoniae* B) NF-κB activation. C) ISGF3 activation.
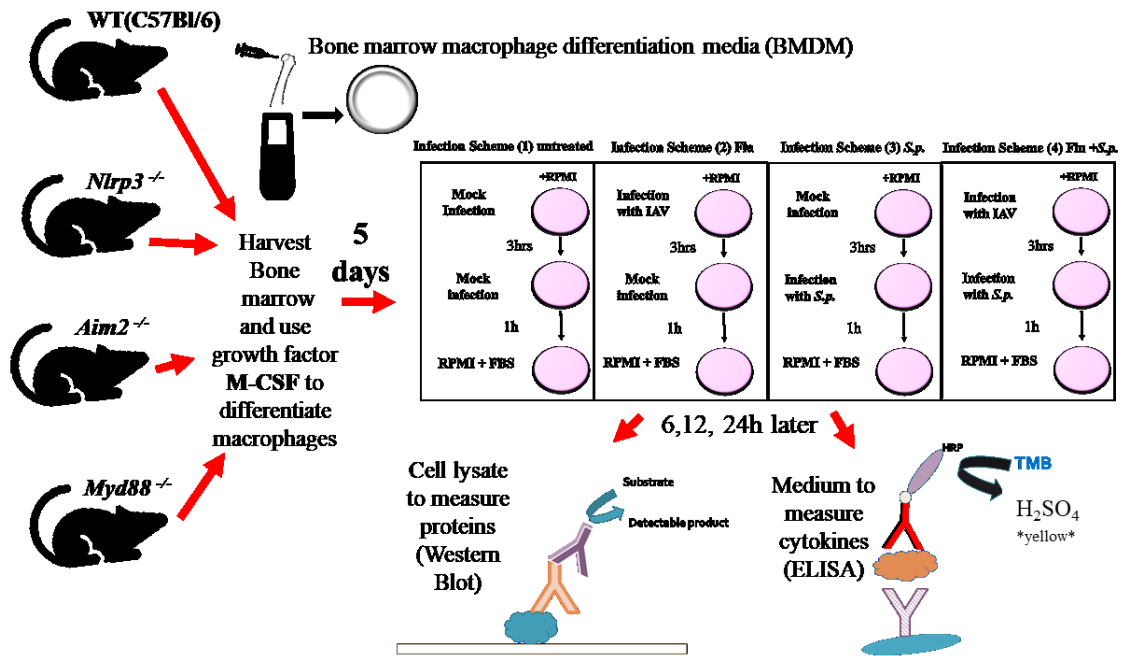
Figure 2. *In vitro* infection scheme. To analyze the proposed signaling pathways we obtained bone marrow from genetically modified mice which are missing a gene important to the pathway mentioned previously. We harvested bone marrow from these mice and made macrophages, then we plated these macrophages and infected them with either influenza, *S. pneumoniae* or both. Finally, we collected the samples usually after 24 hrs and analyzed different proteins and cytokines in our proposed pathway using western blotting and ELISA.
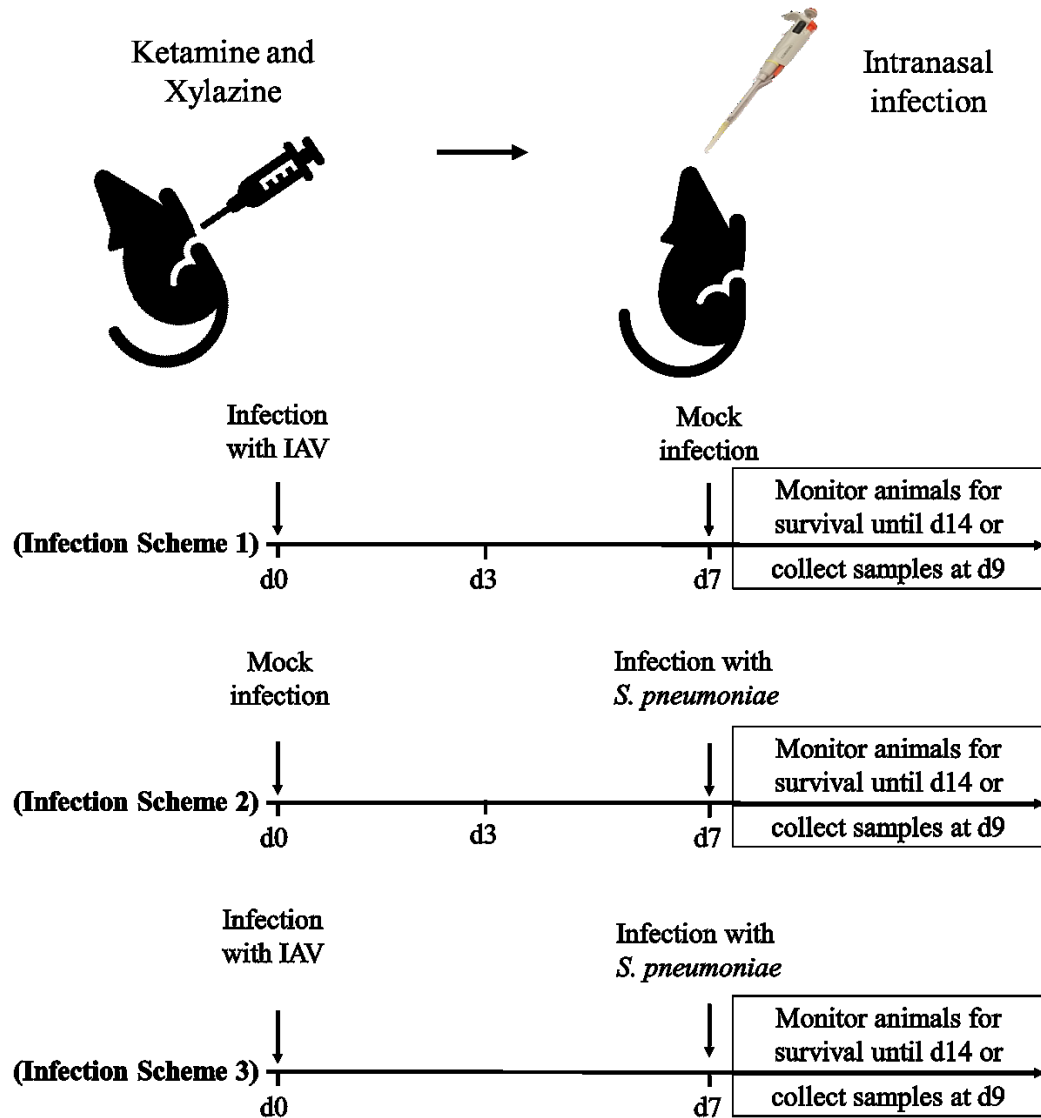
Figure 3. *In vivo* infection scheme. WT and transgenic mice were anaesthetized and infected with one of the three indicated infection schemes intranasally and monitored for weight loss and survival or euthanized and lung samples collected on the indicated day post initial infection.

Drug Treatment
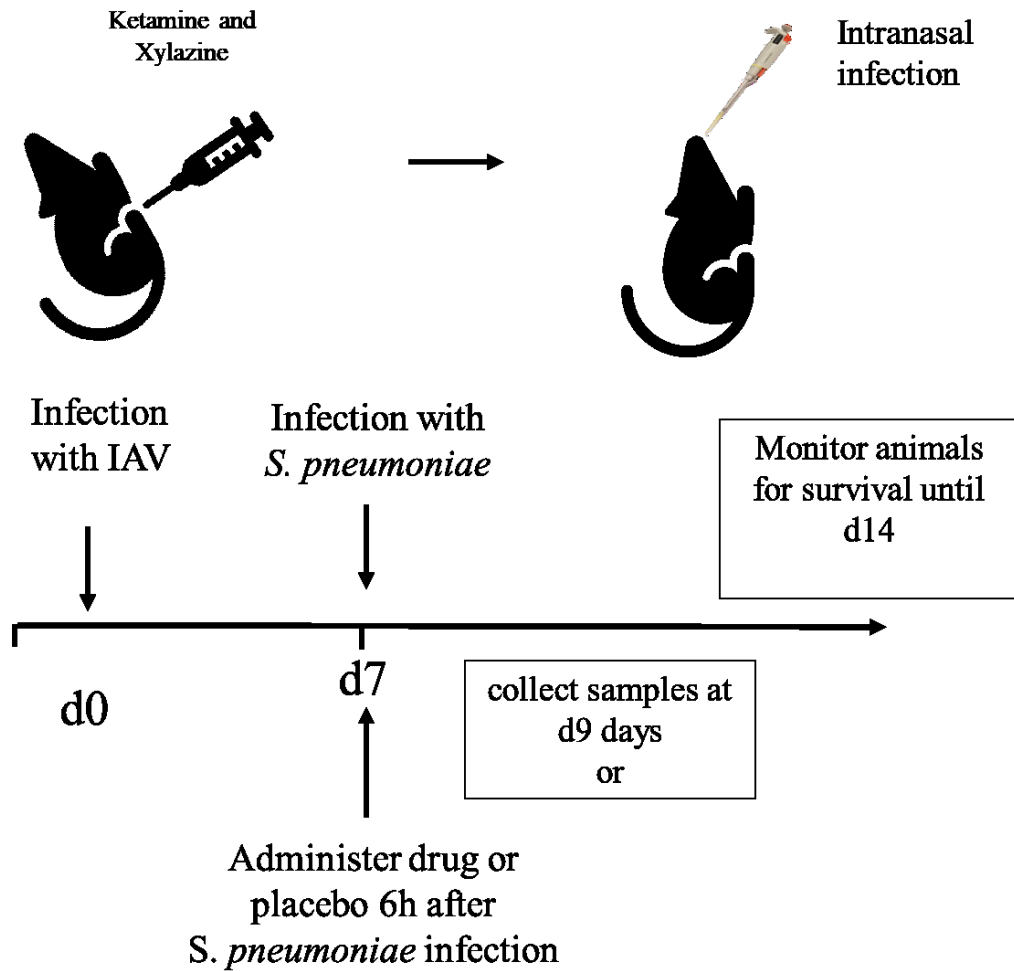
Figure 4. Drug treatment scheme. WT mice were infected and treated with clindamycin or IL-1β neutralizing antibody (IL-1β neut. Ab) or co-treated at the indicated times. Mice were monitored for weight loss and survival or euthanized and lung samples collected on the indicated day post initial infection.
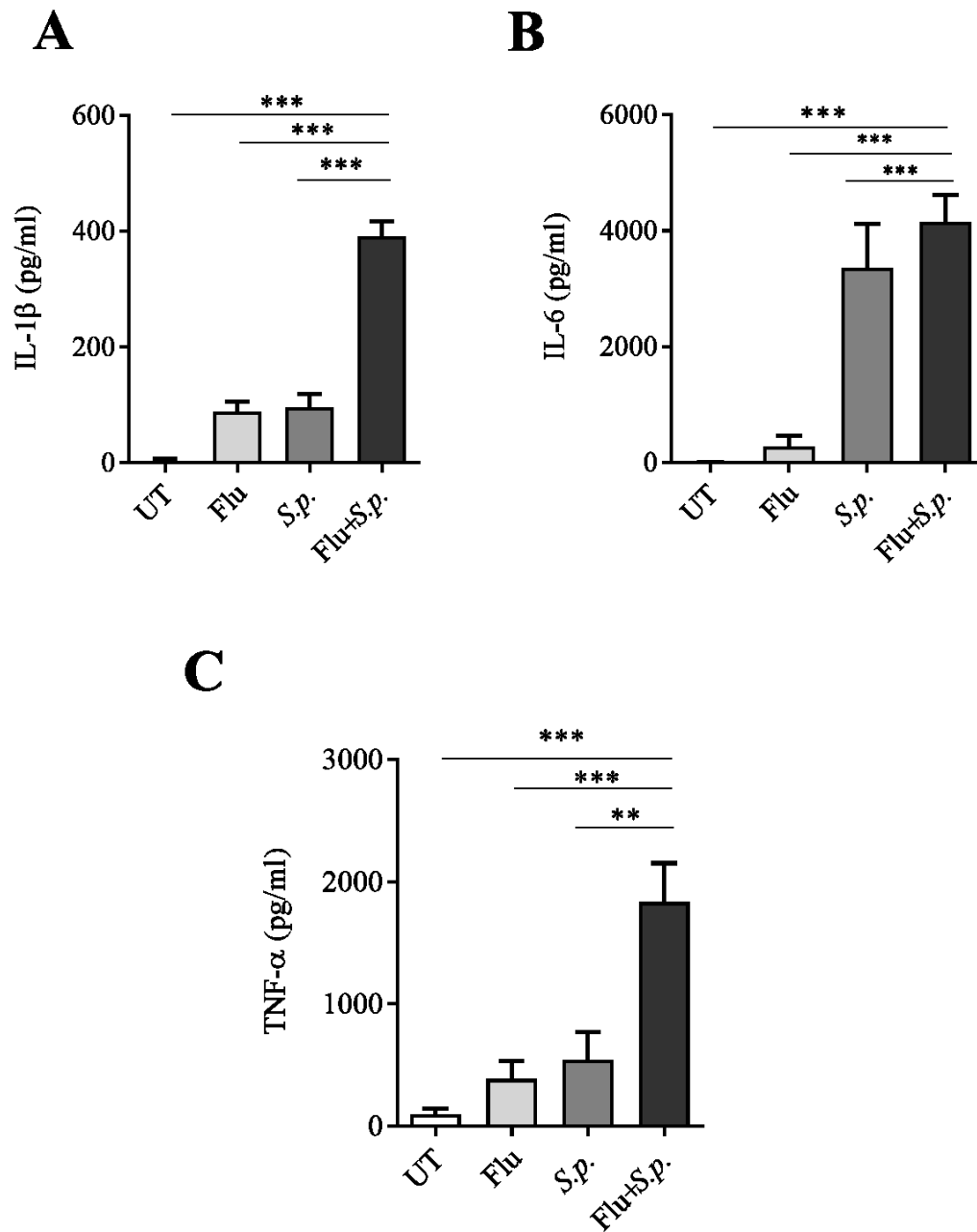
Figure 5. Increased production of cytokine *in vitro* during coinfection. ELISA was ran on samples collected from BMDMs infected with one of the previously stated infection schemes. (A-C) IL-1β, TNF-α and IL-6 concentrations significantly increases during coinfection compared to the uninfected sample. Data represent 2-5 independent experiments using n=2 per experiment. One-way ANOVA using Tukey's post hoc analysis was used for statistical comparison. ns: not significant, p values: <0.05 (*), <0.01 (**), <0.001 (***).
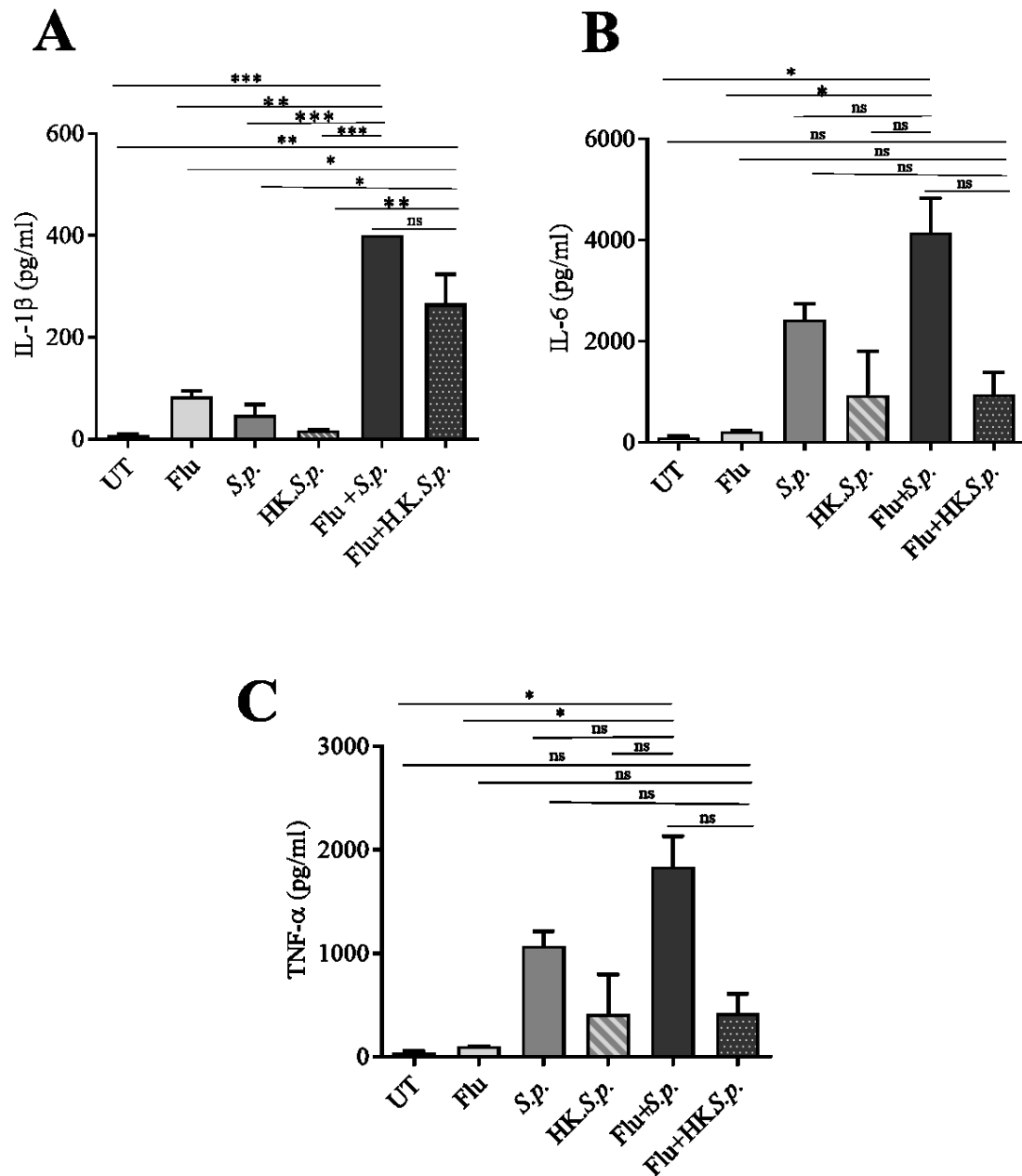
Figure 6. IL-1β is partially dependent on bacterial growth. (A-C).The effect of heat killed *S. pneumoniae* on cytokine production were examined by infecting BMDMs with one of the indicated infection schemes and performing ELISA for IL-1β, TNF-α and IL-6 on samples collected 24 h post-infection. Data represent 2-5 independent experiments using n=2 per experiment. One-way ANOVA using Tukey's post hoc analysis was used for statistical comparison. ns: not significant, p values: <0.05 (*), <0.01 (**), <0.001 (***).

A
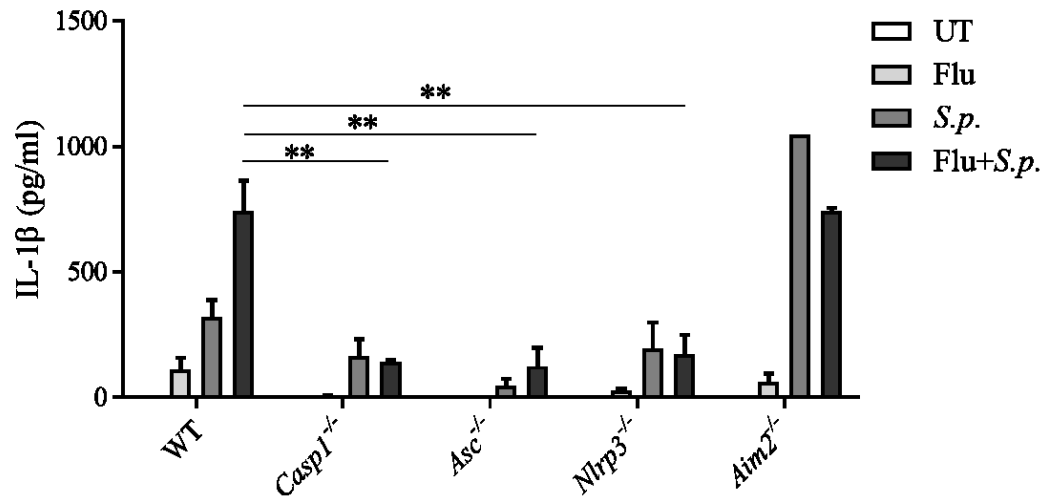
B
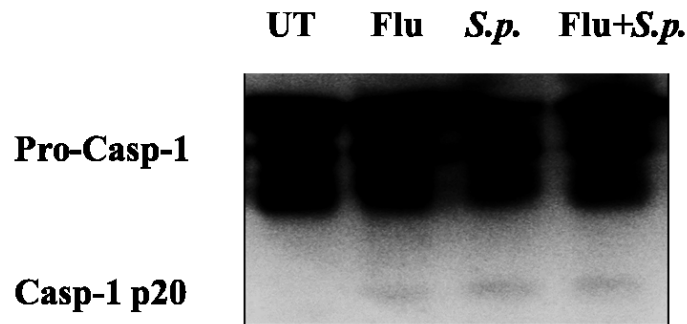
Figure 7. Overproduction of IL-1β is not associated with enhanced inflammasome activation. A) BMDMs from the indicated genotype of mice were infected with a single pathogen or coinfected. Samples collected 24 h post-infection were analyzed by ELISA. Two-way ANOVA using Dunnett's post hoc analysis was used for statistical comparison. p values: <0.05 (*), <0.01 (**), <0.001 (***). B) Protein levels of pro-caspase-1 and active caspase-1p20 were measured using Western blot analysis from BMDMs infected as indicated for 24 h. Actin was used as a control.
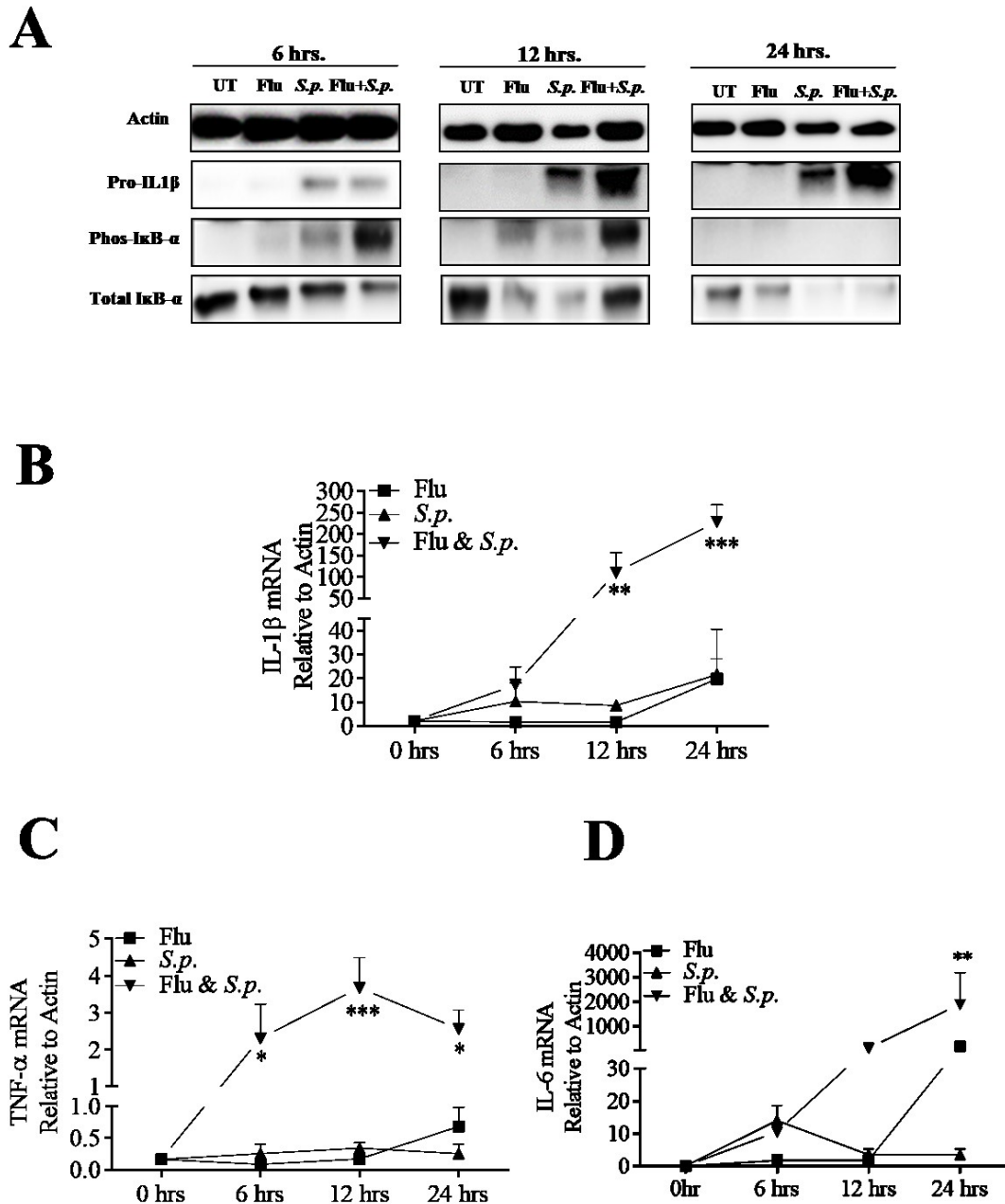
Figure 8. Overproduction of IL-1β is NF-κB dependent. (A) Protein levels of pro-IL-1β, phosphorylated IκB-α and total IκB-α were measured using Western blot analysis from samples collected at 6, 12, or 24 h after the indicated infection. Actin was used as a control. (B-D) mRNA from BMDMs samples collected at 6, 12, or 24 h post-infection with the indicated pathogens were examined for IL-1β, IL-6, and TNF-α gene expression by qRT-PCR. IL-1β mRNA was normalized relative to β -Actin. One-way ANOVA using Tukey's post hoc analysis was used for statistical comparison. p values: <0.05 (*), <0.01 (**), <0.001 (***).
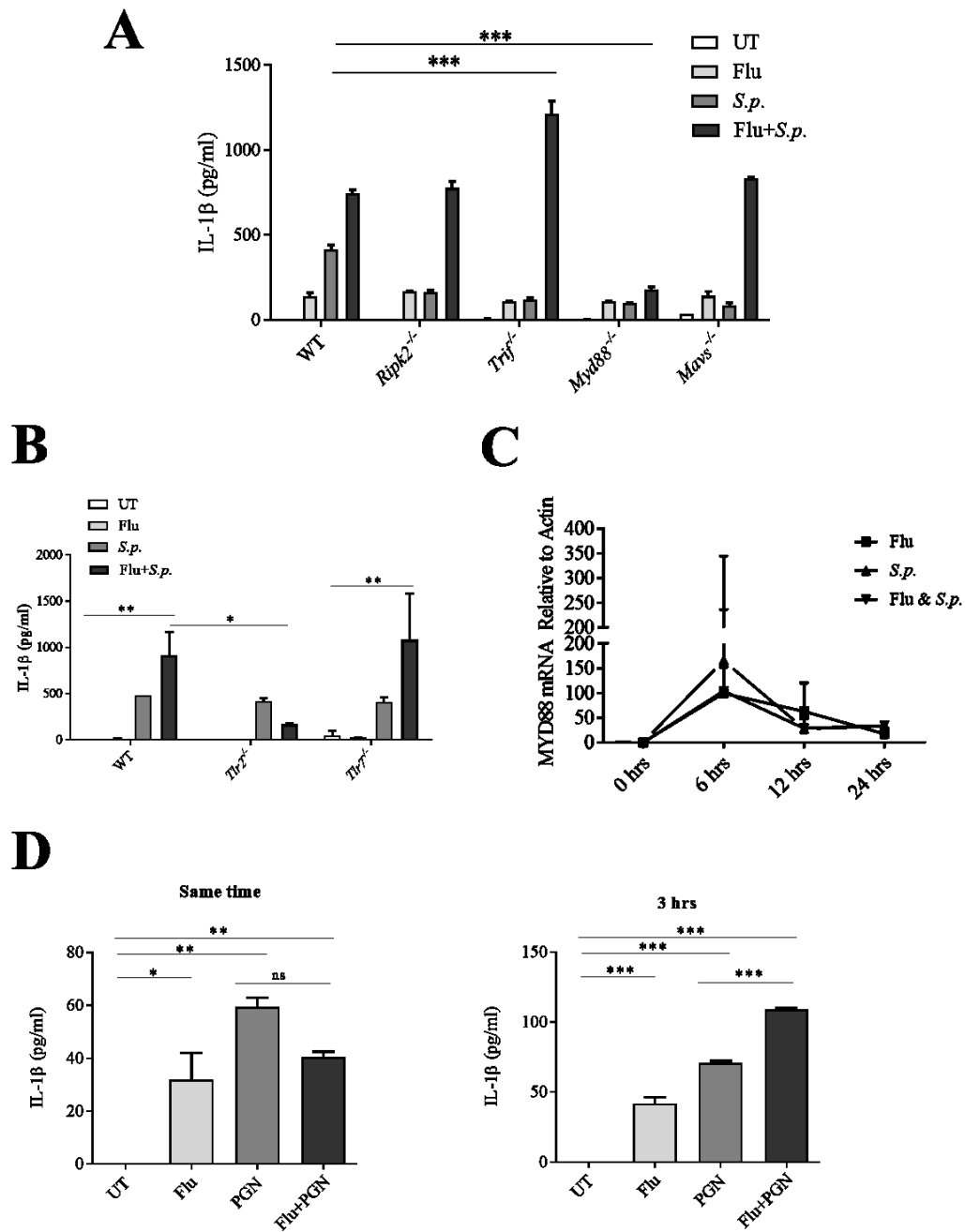
Figure 9. MYD88 is necessary for IL-1β production *in vitro.* A-B) ELISA was ran on samples collected from BMDMs infected with one of the infection schemes. C) mRNA from BMDMs samples collected at 6, 12, or 24 h post-infection with the indicated pathogens were examined for MYD88 gene expression by qRT-PCR. MYD88 mRNA was normalized relative to β -Actin. D) ELISA was run on samples collected from BMDMs infected with one of the infection schemes using Peptidoglycan (PGN) at the same time during coinfection or three hours apart. One-way ANOVA using Tukey's post hoc analysis was used for statistical comparison. p values: <0.05 (*), <0.01 (**), <0.001 (***).
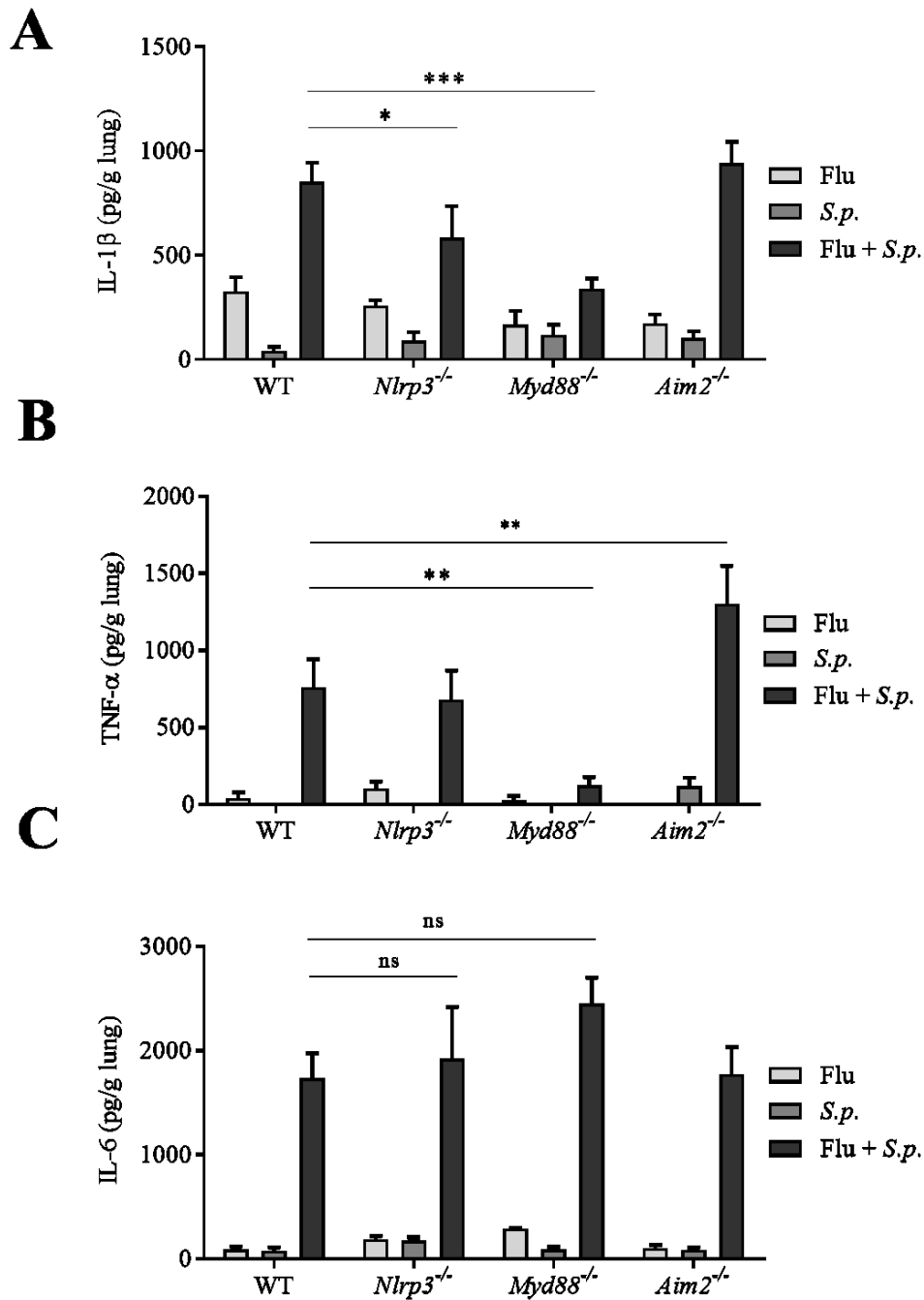
Figure 10. Increased production of IL-1β *in vivo* is dependent on MYD88 and NLRP3. (A-C) Indicated cytokine levels were examined in whole lung homogenates on day 9 post-PR8, day 2 post-*S.p.* or day 2 post-coinfection. Data are representative of two experiments, n=5-7 mice per group per experiment. One-way ANOVA using Tukey's post hoc analysis was used for statistical comparison. ns: not significant, p values: <0.05 (*), <0.01 (**), <0.001 (***).
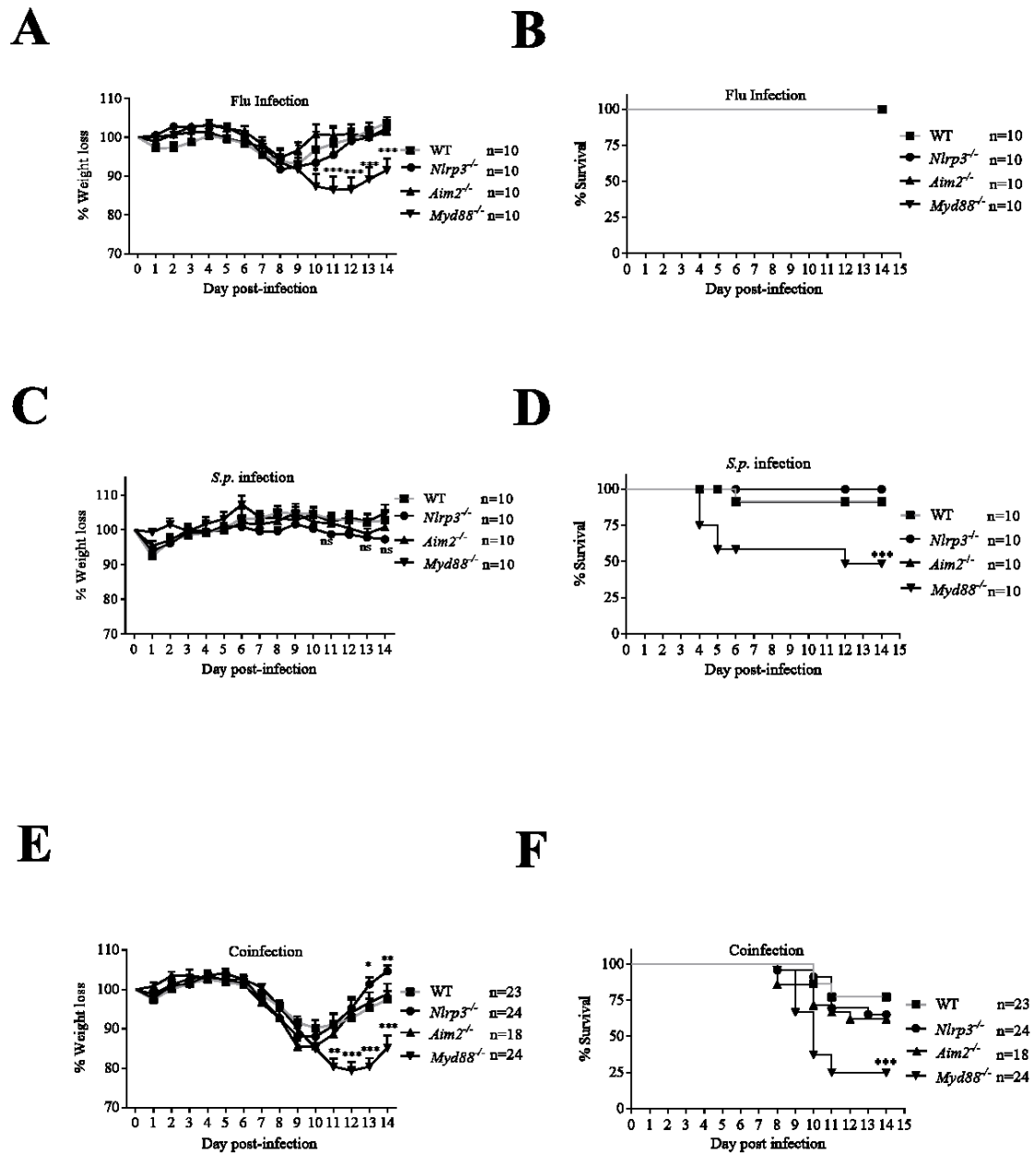
Figure 11. Morbidity and mortality of infected transgenic mice. (A,C,E). Weight loss in mice infected with PR8 alone, *S.p.* alone, or PR8-*S.p.* coinfection. (B,D,F) Mortality in mice infected with PR8 alone, *S.p.* alone, or PR8-*S.p.* coinfection. (A-F) Data are combined from two to three experiments, total n is indicated. Two-way ANOVA using Tukey's post hoc analysis was used for statistical comparison for weight loss and Kaplan-Meier Survival Plot and LogRank Test for survival data. ns: not significant, p values: <0.05 (*), <0.01 (**), <0.001 (***).
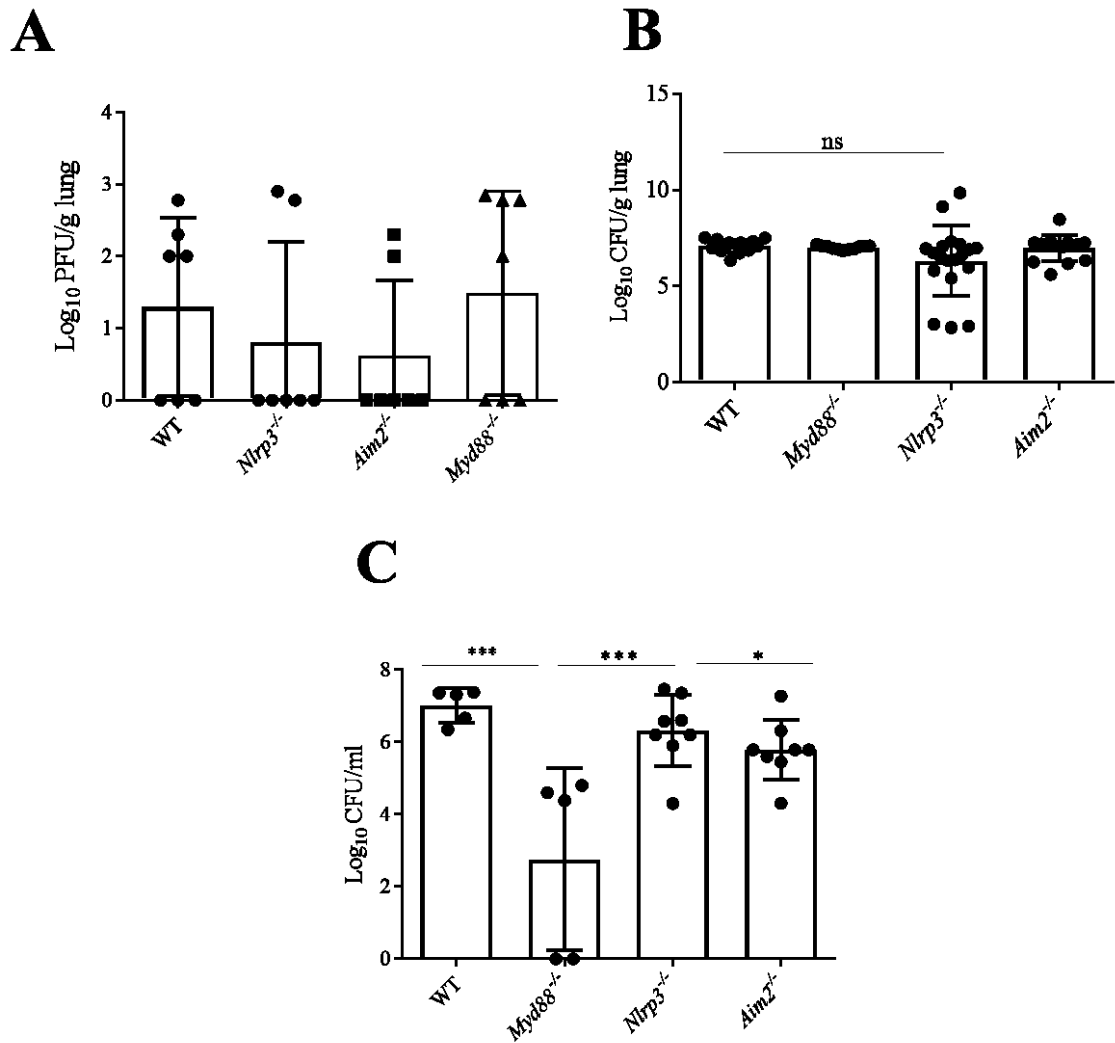
Figure 12. Viral and Bacterial titers in knockout mice. (A-B) Bacterial and viral titers in whole lung homogenates of coinfected mice on day 2 after coinfection. (C) Bacterial titers in blood of coinfected mice on day 2 after coinfection. Data are representative of two-three experiments, n=5-7 mice per group per experiment. One-way ANOVA using Tukey's post hoc analysis was used for statistical comparison (no differences were statistically significant).
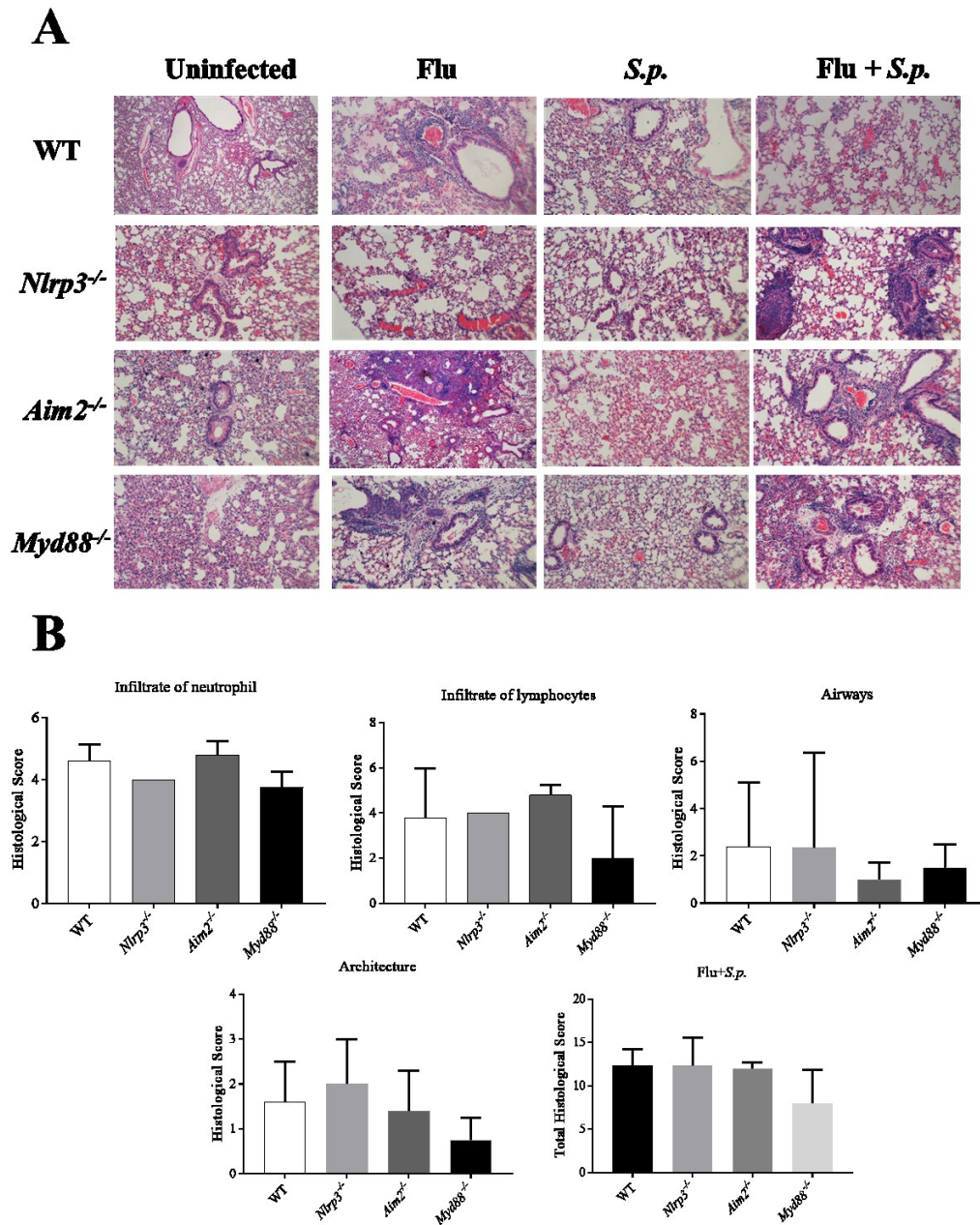
Figure 13. Histopathology of coinfected lungs. (a) Representative lung cross-section stained with H&E (40X). (B) Histological score from cross- sections of coinfected mice lungs obtained on day 2 after coinfection stained with H&E. Data are representative of two-three experiments, n=5-7 mice per group per experiment. One-way ANOVA using Dunn post hoc analysis and the Kruskal-Wallis test was used for statistical comparison. (no differences were statistically significant).
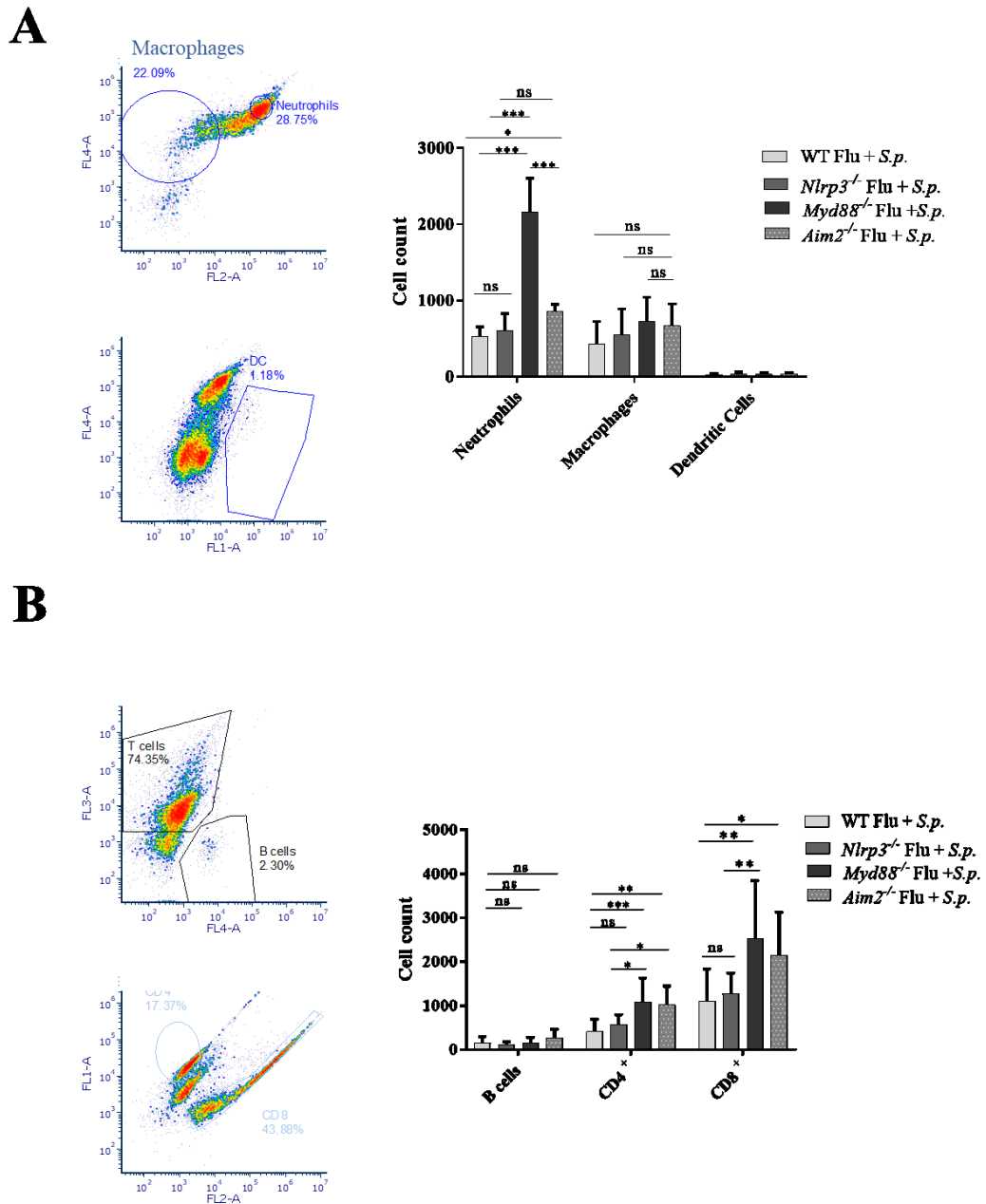
Figure 14. Immune cell population during infection schemes with transgenic mice. Coinfected lungs of 9-14 mice were homogenized and analyzed by flow cytometry. A) Antibodies to detect neutrophils, macrophages and dendritic cells were used. B) B cell, CD4 T cell and CD8 T cell population in WT and knockout mouse lungs were analyzed. One-way ANOVA using Tukey's post hoc analysis was used for statistical comparison. ns: not significant, p values: <0.05 (*), <0.01 (**), <0.001 (***).
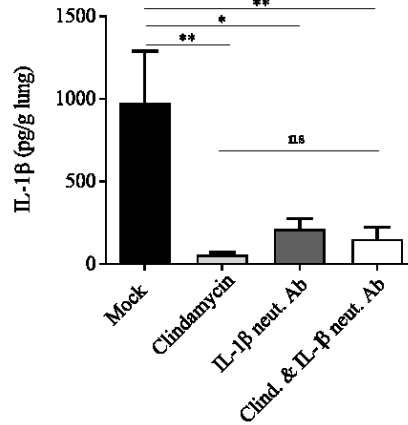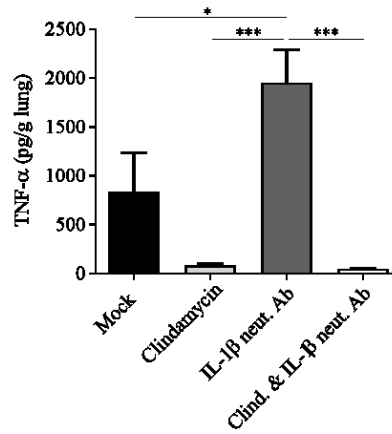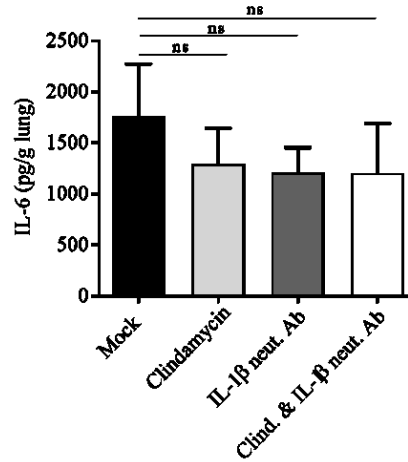
Figure 15. Combination treatment with clindamycin and IL-1β neutralizing antibody in mice. (A-C) Indicated cytokines were examined in whole lung homogenates on day 2 post-coinfection (day 9 post-PR8) by ELISA (A-C) Data are representative of two experiments, n=3-7 mice per group per experiment. One-way ANOVA using Tukey's post hoc analysis was used for statistical comparison.
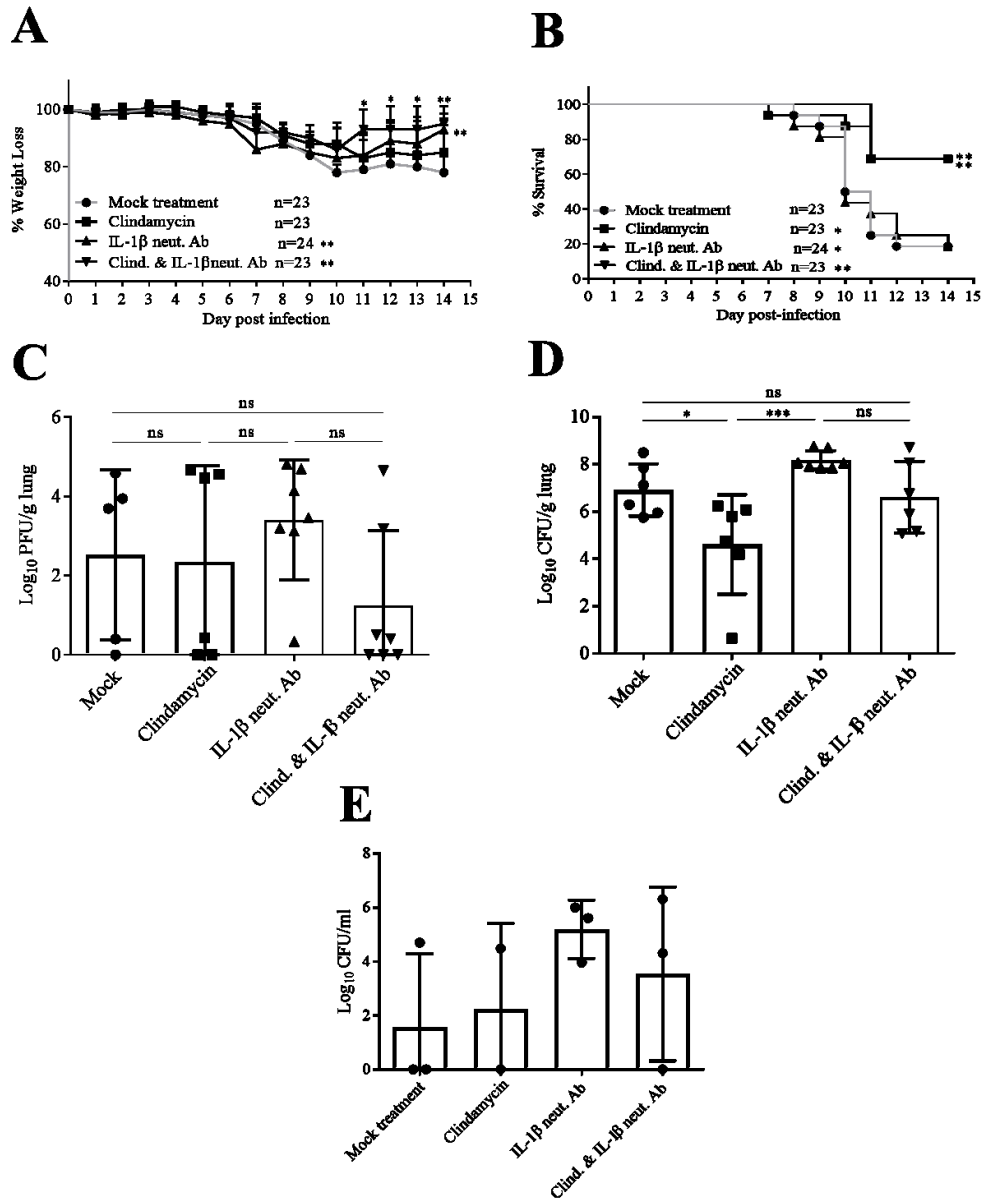
Figure 16. Morbidity and mortality during treatment. (A-B) Weight loss and mortality in WT mice coinfected and then treated with the indicated antibiotic and/or IL-1β neutralizing antibody. (C-D) Bacterial and viral titers in whole lung homogenates of coinfected mice on day 2 post-coinfection. (A-B) Data are combined from two experiments, total n is indicated. Two-way ANOVA using Tukey's post hoc analysis was used for statistical comparison for weight loss and Kaplan-Meier Survival Plot and LogRank Test for survival data. ns: not significant, p values: <0.05 (*), <0.01 (**), <0.001 (***). (C-D) Data are representative of two experiments, n=3-7 mice per group per experiment. One-way ANOVA using Tukey's post hoc analysis was used for statistical comparison.
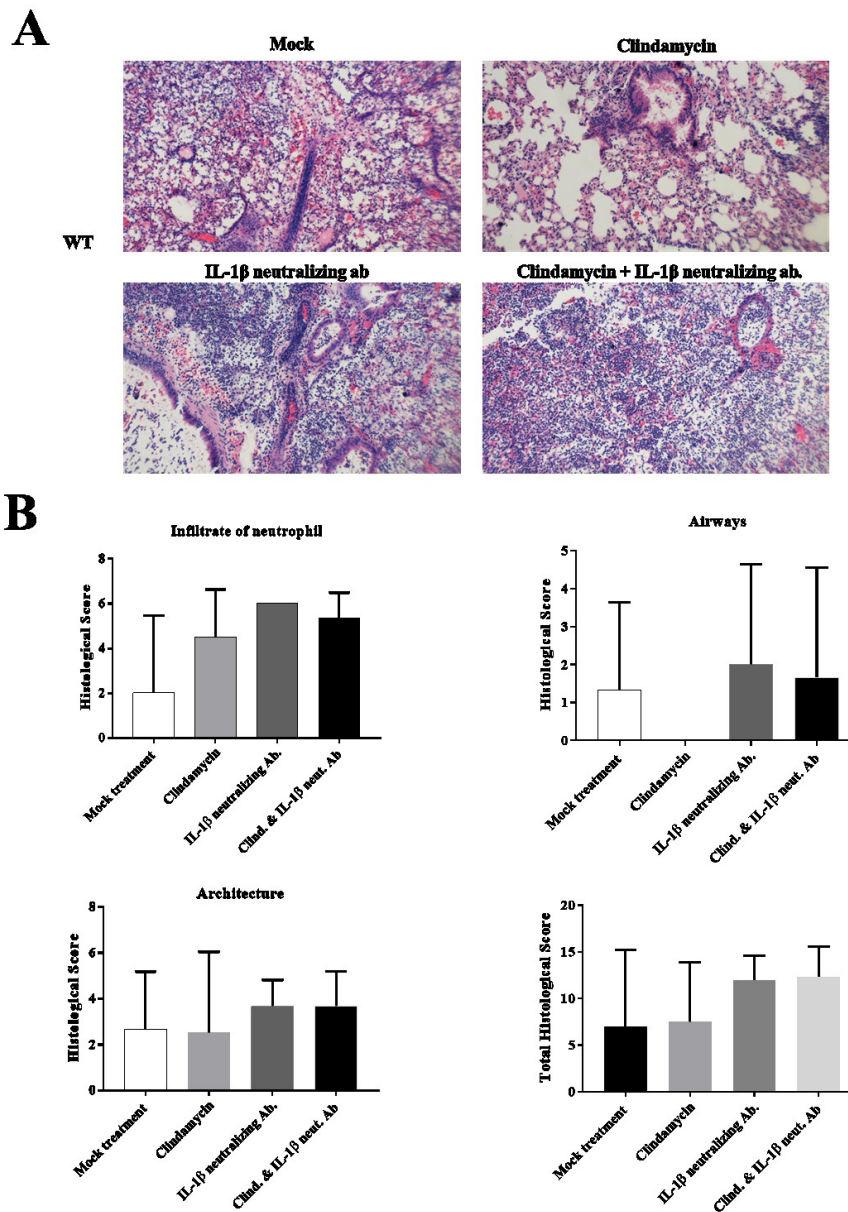
Figure 17. Histopathology of coinfected lungs treated with an antibiotic, a neutralizing antibody or combined treatment. (a) Representative lung cross-section stained with H&E (10X). (B) Histological score from cross- sections of coinfected mice lungs obtained after treatment and on day 2 after coinfection stained with H&E. Data are representative of two-three experiments, n=5-7 mice per group per experiment. One-way ANOVA using Dunn post hoc analysis and the Kruskal-Wallis test was used for statistical comparison. (no differences were statistically significant).
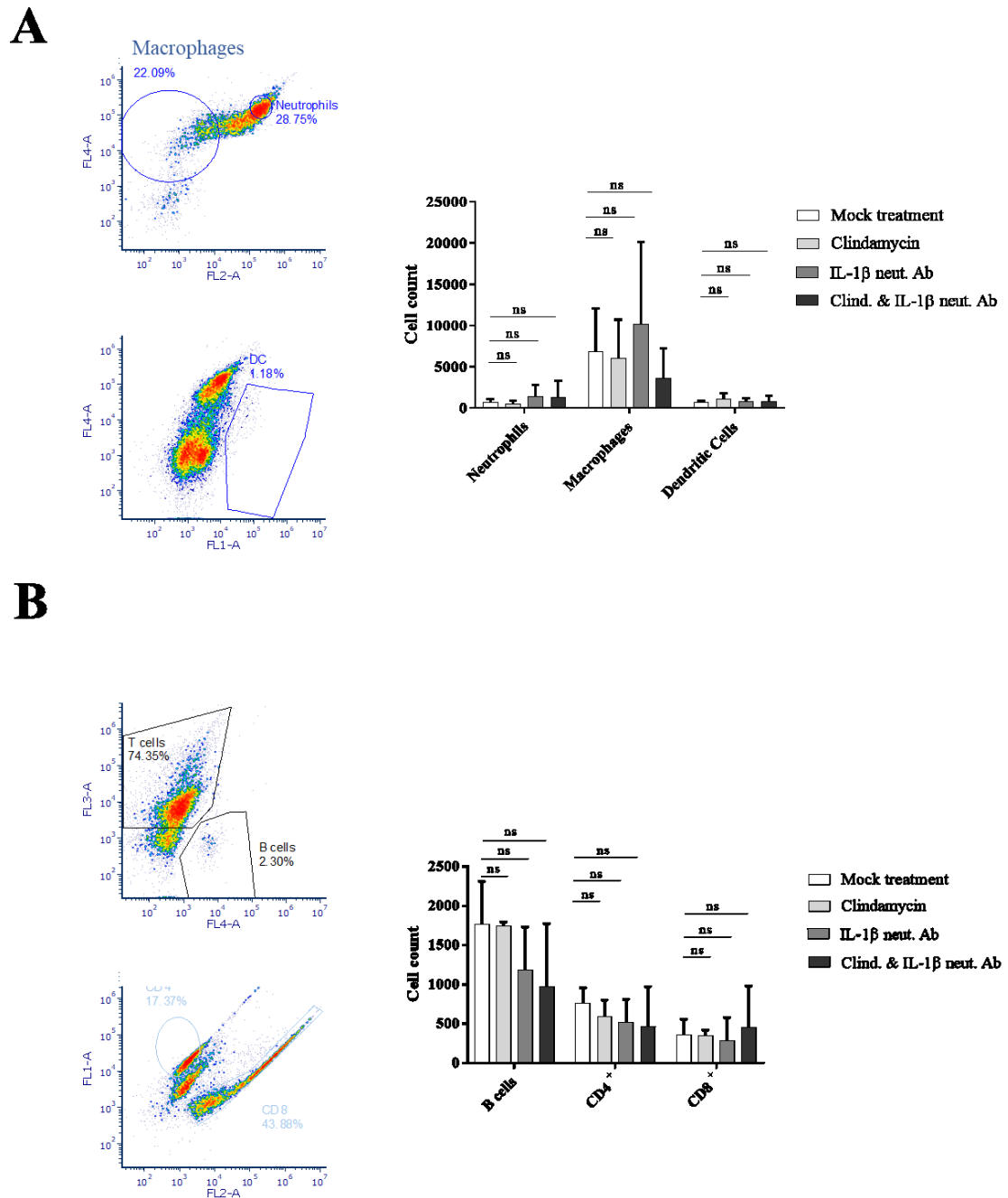
Figure 18. Immune cell population among drug treatments. Coinfected lungs of 9-14 mice were homogenized and analyzed by flow cytometry. A) Antibodies to detect neutrophils, macrophages and dendritic cells were used. B) B cell, CD4 T cell and CD8 T cell population in WT mouse lungs were analyzed. The changes of cell population under different treatments were studied.
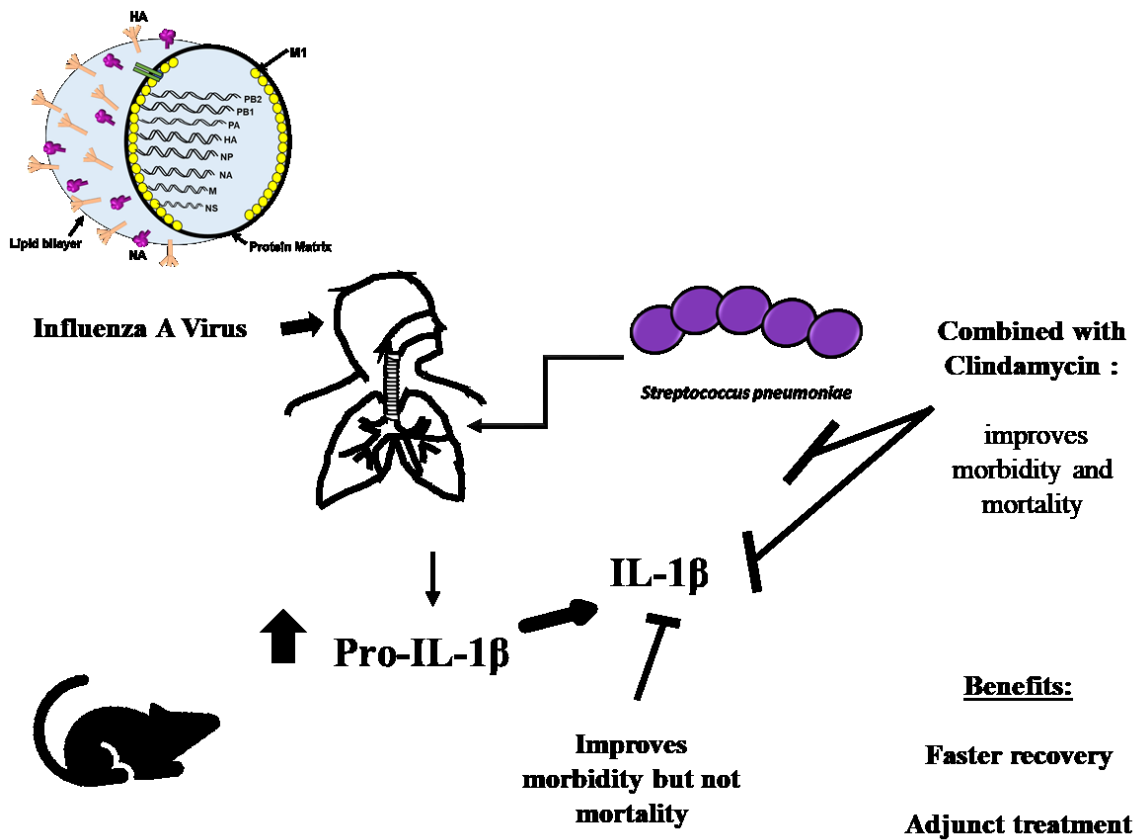
Figure 19. Influenza A Virus and *Streptococcus pneumoniae* coinfection and IL-1β involvement. During the coinfection of IAV and *S.p.* it is well known that IAV aids the bacteria by damaging epithelial layers, suppressing the respiratory burst of leukocytes, impeding bacterial clearance, depleting alveolar macrophages and dysregulating neutrophils. An overactive immune response results from *S.p.* infecting the host. This results in the increase production of the cytokine IL-1β. This increase is not due to enhanced activation of the inflammasome enzyme Caspase-1 or bacterial overgrowth. It is due to enhanced priming of the transcription faction NF-κB which results in elevated levels of pro- IL-1β. Using a neutralizing antibody to block IL-1β only helps improve morbidity and mortality in mice if combined with the antibiotic Clindamycin.